

INTERNALS – ENVIRONMENTAL EFFECTS ON IASCC SUSCEPTIBILITY OF INTERNALS II

TASK 4.3: EFFECTS OF THE ENVIRONMENT ON THE OXIDE PROPERTIES

4.3.1 THE EFFECT OF **CHEMICAL TRANSIENTS** ON THE OXIDE PROPERTIES

4.3.2 THE EFFECT OF **HYDROGEN** ON THE OXIDE PROPERTIES

4.3.3 THE EFFECT OF **CHEMICAL SPECIES (B, LI)** ON THE OXIDE PROPERTIES

S. Merino, G. de Diego and C. Maffiotte



This project received funding under the Euratom research and training programme 2014-2018 under grant agreement N° 661913

1. Objective
2. Background
3. Experimental Procedure
 1. Material Characterization
 2. Test Matrix
 3. Oxidation test
 4. Oxide layer characterization
4. Discussion and Results
5. Summary

1.- OBJECTIVE



- The objective of this work is **to characterize the protective oxide layer** formed on AISI 316L stainless steel in PWR primary water and to determine if the differences of the environment (**transients, hydrogen and B/Li ratio**) modify the microstructure and composition of this protective layer in order to understand the susceptibility to SCC.



2.-BACKGROUND



- ❑ Austenitic stainless steels form a chromium oxide (Cr_2O_3) on surface at low temperature what could be denominated as “ideal passive or protective oxide layer”.
- ❑ At high temperatures and depending on the environment, other different oxides may form at the surface of the alloy.
- ❑ Primary water of a PWR has a strong influence on the oxide film properties and it is linked to the oxidation kinetics.
- ❑ Under these chemical water conditions, the protective oxide layer of the austenitic stainless steels surface can evolve to different microstructure¹.

¹ EPRI, 2015 TECHNICAL REPORT **3002005478** . Program on Technology Innovation: Review of Oxidation and Surface Film Formation Studies on Austenitic Alloys in Light Water Reactor Coolants



3. Experimental Procedure

1. Material Characterization
2. Test Matrix
3. Oxidation test
4. Oxide layer characterization

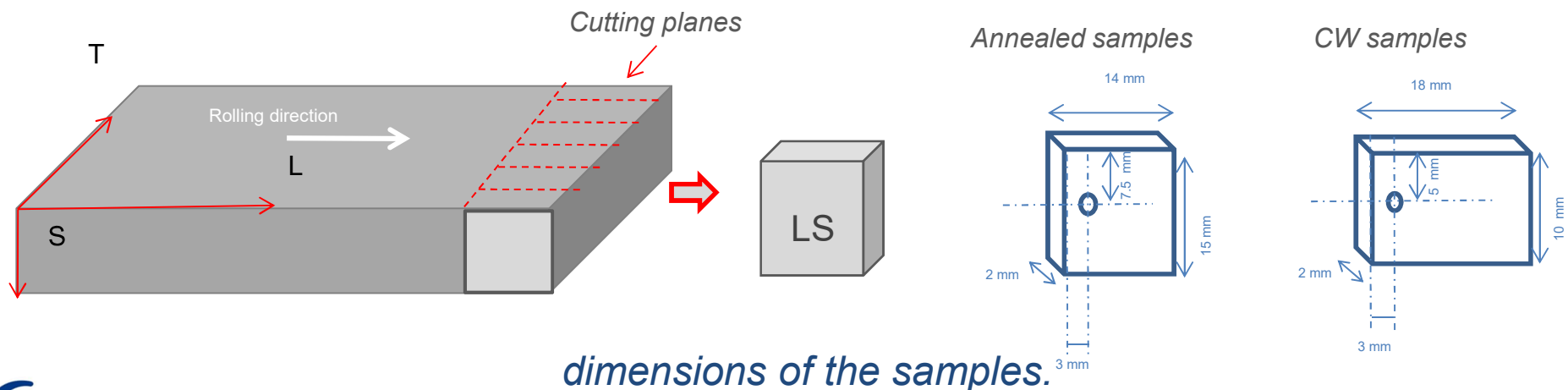
3.1 Materials Characterization



□ Austenitic stainless steels AISI 316L

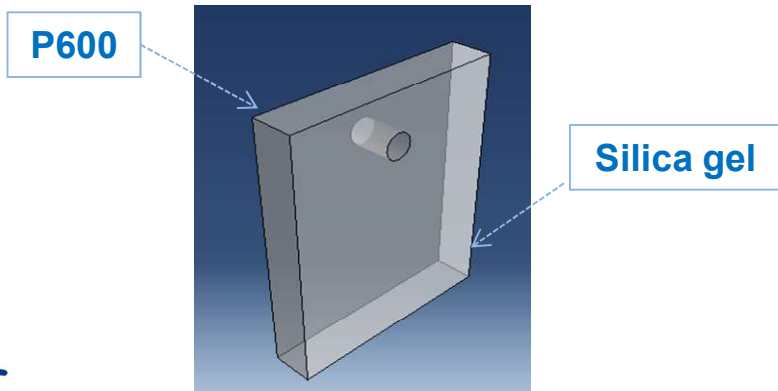
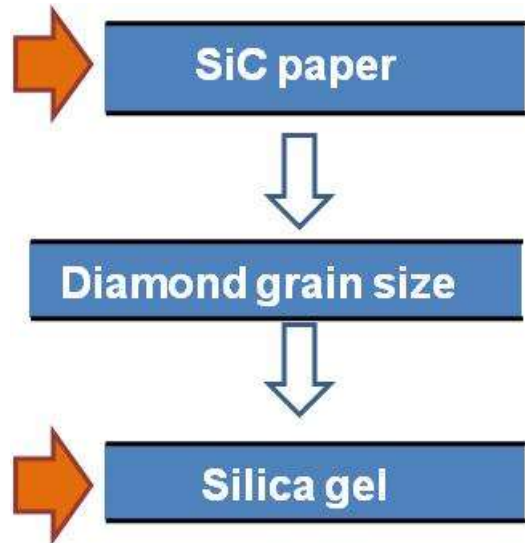
% Wt.	C	Cr	Mn	Mo	N	Ni	P	S	Si
316L-Certif.	0.016	16.822	1.84	2.086	0.025	10.170	0.026	0.003	0.641

- The material was tested in two conditions:
Annealed and 30% Cold Worked by rolling
- The plate was cut in LS direction

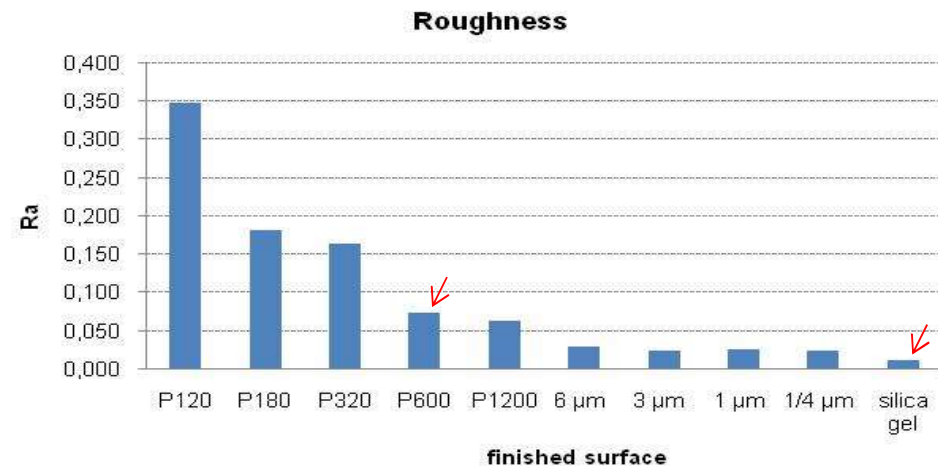


3.1 Materials Characterization

Two Surface finished

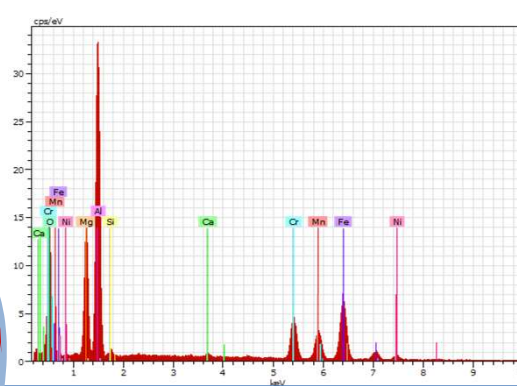
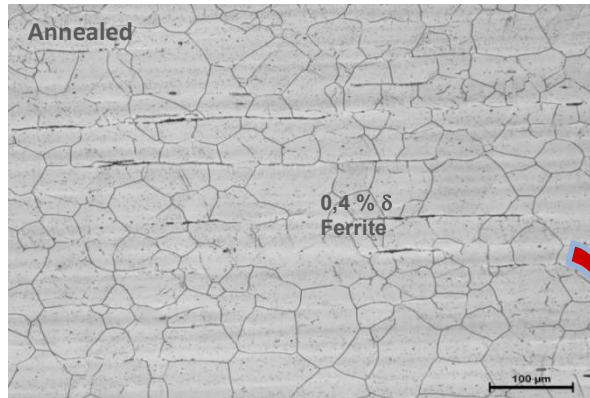


- The surface preparation was performed by mechanical grinding and polishing.
- All the samples were finished with silica gel in one of the sides. The other side was ground (P600).
- The roughness ground value (Ra) is almost three times greater than the polished value.
- In this way is possible to determine differences of the oxide formed between ground and polished surface.

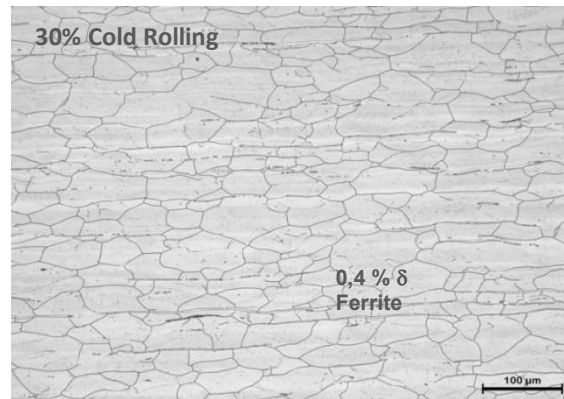


3.1 Materials Characterization

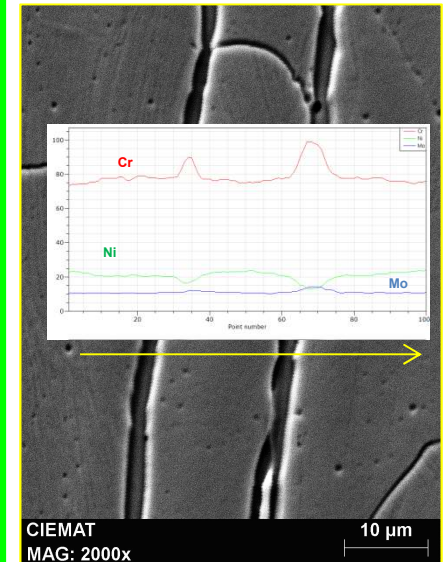
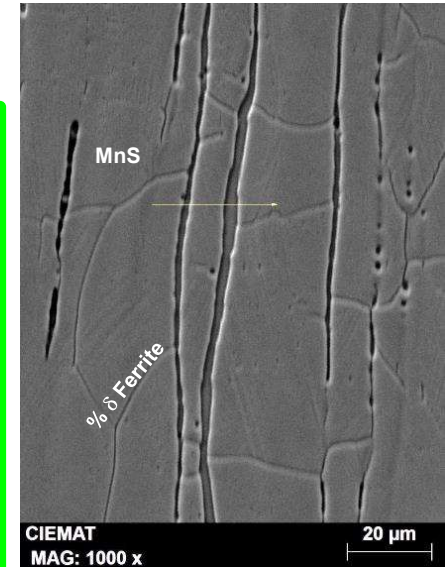
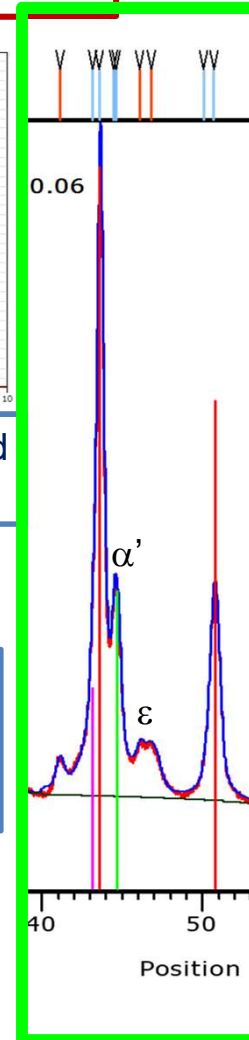
□ The microstructure of the samples shows equiaxed grains with no evidence of carbide precipitation along the grain boundaries.



MnS and Aluminium and Magnesium oxide are present



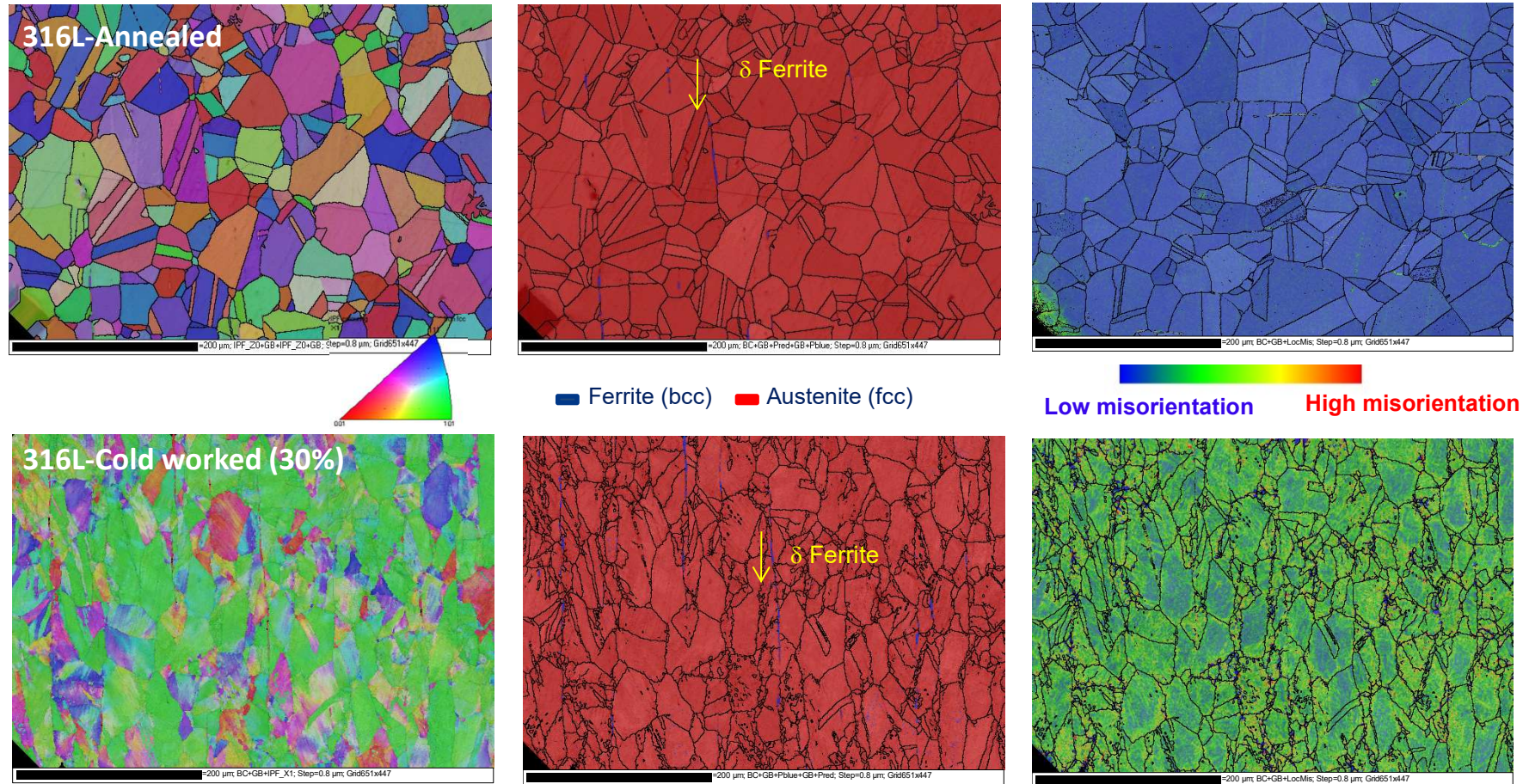
Cold work induced ϵ and α' martensitic transformation by plastic strain



	HV	G(ASTM)	d (μm)	(Ferritoscope)
316L annealed	145	5.35 ± 0.18	45	0.4 (δ)
316L30% CW	272	5.03 ± 0.43	53	3.5 (δ + ε + α')

3.1 Materials Characterization

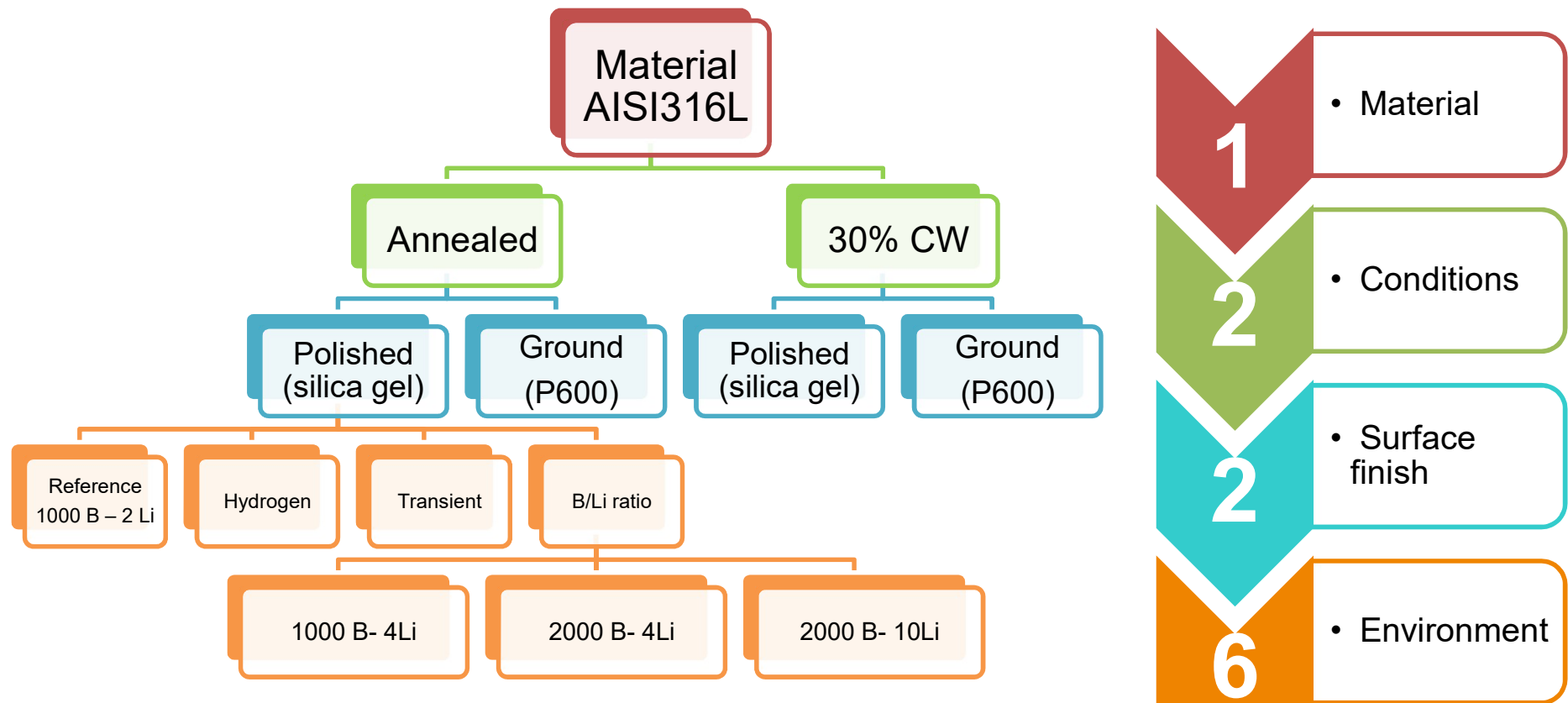
EBSD was performed before oxidation test to identify the grains boundaries, twins and δ ferrite in order to determine the effect of grain orientation in the oxide layer.



- In AISI 316 austenitic stainless steel, the cold work increases the microtexture (101)
- Green-yellow indicates a higher misorientation in CW material.



3.2 Test matrix



- 8 samples/conditions = 16 samples/test
- 6 tests (1000 h) – 96 samples – 2 surfaces



3.3 Oxidations tests

- The environment conditions were chosen in order to simulate as close as possible the complexity of the operating conditions in PWR.

Reference test: dynamic loop – 1000 h
325 °C - 1000 ppm B - 2 ppm Li - 30 cc/kg H₂

TASK
4.3.1

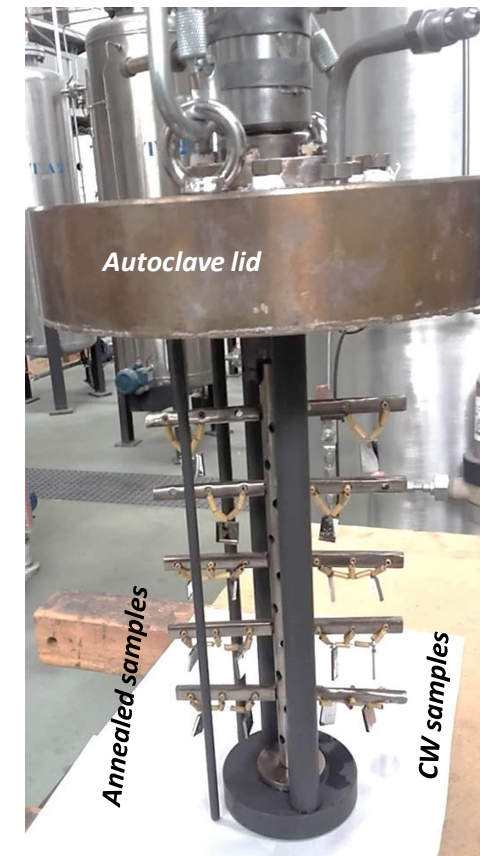
Transient

TASK
4.3.2

Hydrogen

TASK
4.3.3

B/Li ratio



samples scheme before the test

3.3 Oxidations tests

TASK
4.3.3

B/Li ratio

- ❑ The main chemical parameters of the PWR primary coolant are boric acid, lithium hydroxide and hydrogen concentrations, and the resulting pH level.
- ❑ Li and B concentrations can vary during the operation of the power plant.
- ❑ The main objective of this subtask is to investigate separately the influence of chemical species (B and Li) on the properties of the oxide layers formed in PWR primary water.

	B (ppm)	Li (ppm)	pH	Cond.(μ S/cm)
Reference	1000	2	6.6	22
Li effect	1000	4	7.0	43
B effect	2000	4	6.2	46
Li effect	2000	10	6.7	116

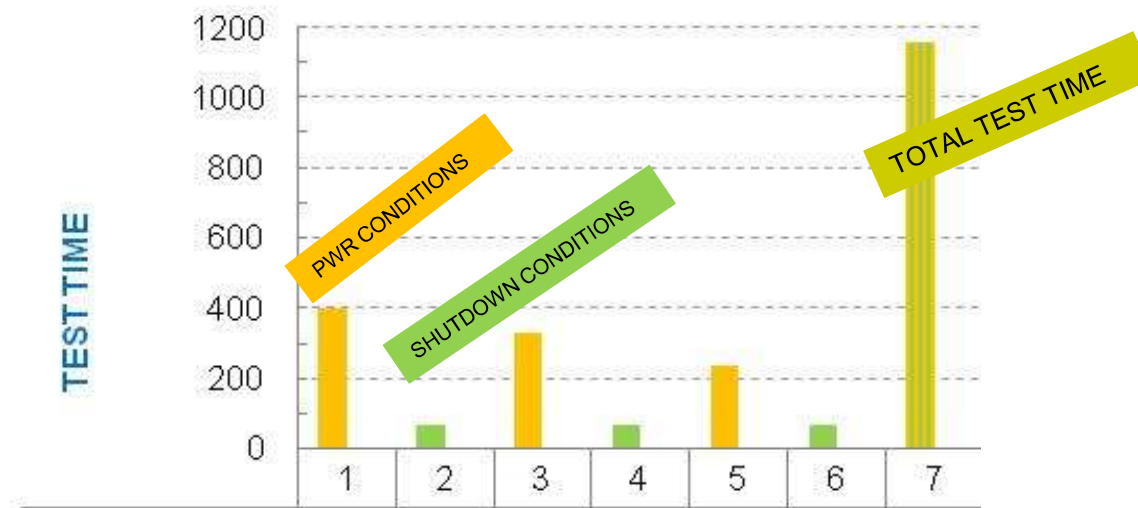
Oxidation tests are performed in dynamic loop – 1000 h-325 °C - 30 cc/kg H₂

3.3 Oxidations tests

TASK
4.3.1

Transient

- ❑ Shutdown conditions were studied with a drastic environmental change from reducing to oxidizing.
 - ❑ PWR (reference conditions) (325 °C - 1000 ppm B-2 ppm Li - 30 cc/kg H₂ - 300 h) Oxidation are performed in dynamic loop.
 - ❑ Shutdown conditions (60 °C -2000 ppm B – 0 ppm Li – pH = 4,6 – air- 67 h)
- ❑ These two steps will be repeated until accumulating 1000 hours.



SOTERIA Final Workshop | 25-27 June 2019 | Miraflores de la Sierra

3.3 Oxidations tests

TASK
4.3.2

Hydrogen

- ❑ Hydrogen cathodic charged samples were used to correlate the SCC susceptibility to the content of hydrogen adsorbed.
- ❑ The Vickers microhardness (HV) of the samples was measured before and after cathodic charge. Hardness was increased due to hydrogen induced deformation. The hardening decrease with depth.
- ❑ After cathodic charge, the specimens were tested in reference conditions at high temperature.
- ❑ Residual and diffusible hydrogen was measured by hot extraction after cathodic charge and after oxidation tests.

After cathodic hydrogen charging ϵ martensite and α' martensite phases are detected by GIXRD



316L (ASTM E112-96)	before	after cathodic charge			
	HV (1000g)	HV (1000g)	HV (500g)	HV (200g)	HV (50g)
	143.7	217.5	253.8	354.1	381.3

3.4 Oxide layer characterization



1. **Oxide surface:** characterization by SEM and Profilometry.
2. **Thickness and composition:** analysis of the oxide layers by Auger, XPS, XRD and Raman Spectroscopy.
3. **Cross-section characterization:** analysis by SEM and TEM.

The Information obtained by different techniques is complementary and provides a comprehensive understanding of the oxide layers formation.



Location of oxide layer alterations which can give rise to crack initiation

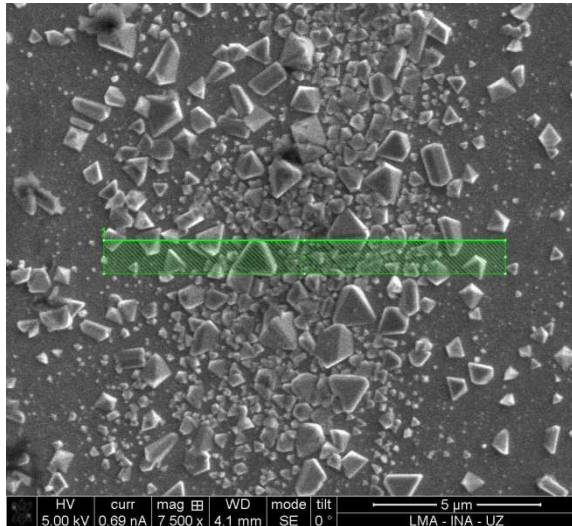


4. Results and discussion

Results: REFERENCE CONDITIONS-Auger



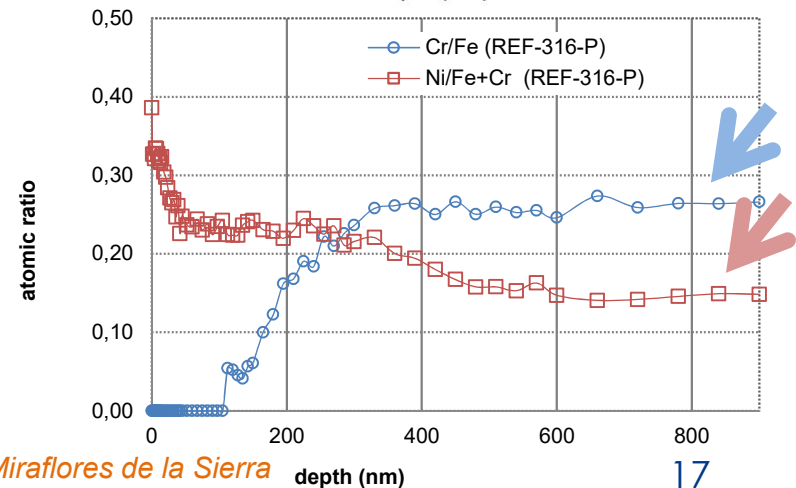
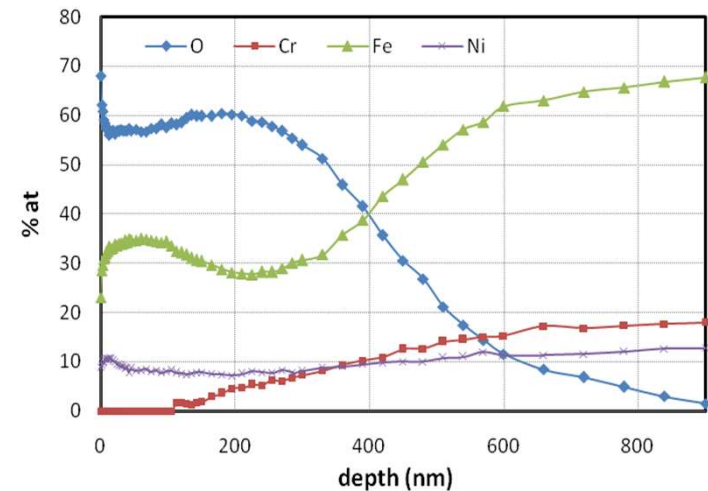
- The oxide layer formed in reference conditions was characterized in order to obtain a “reference oxide layer” and to compare with the other ones obtained in different environments.
- **Thickness and composition:** analysis of the oxide layers by Auger Spectroscopy



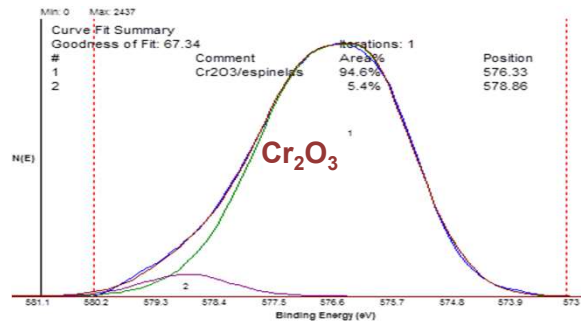
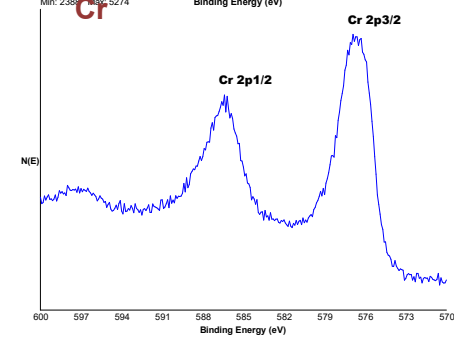
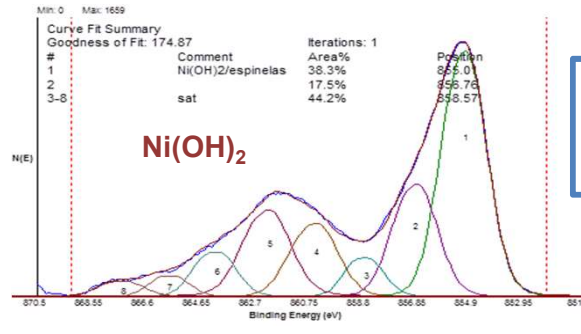
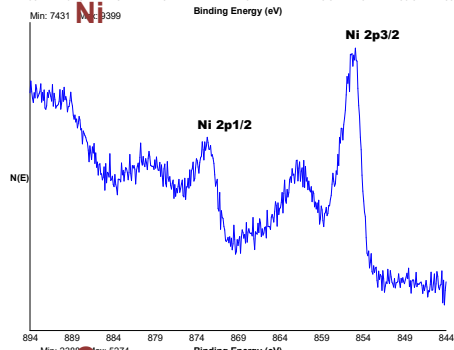
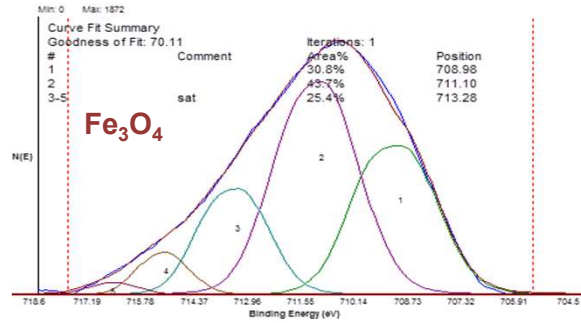
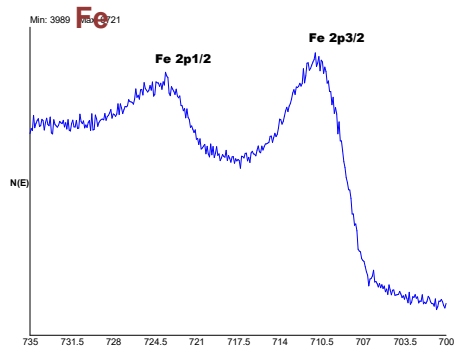
□ Outer layer Fe-rich and below this phase appears a Fe/Cr/Ni mixed spinel.

□ The thickness is determined when Cr/Fe and Ni/Fe+Cr are close to nominal values

Nominal composition	Cr/Fe	Ni/(Fe+Cr)
	0.25	0.12

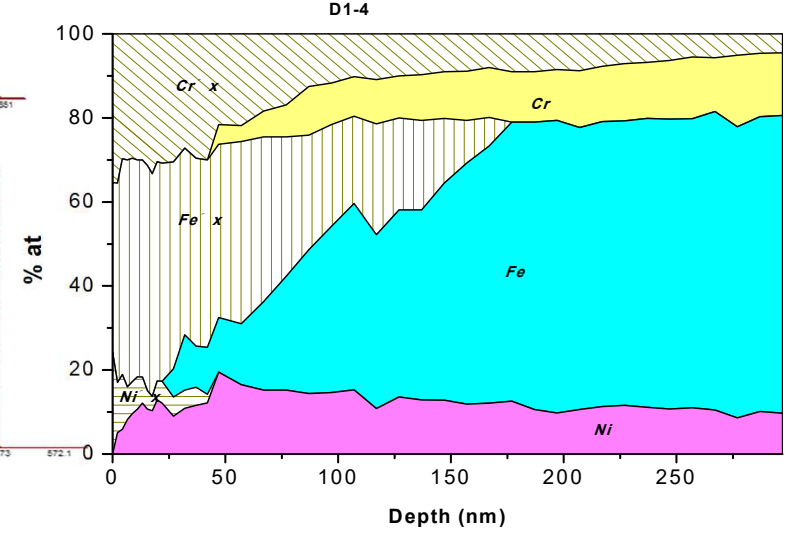


Results: REFERENCE CONDITIONS-XPS

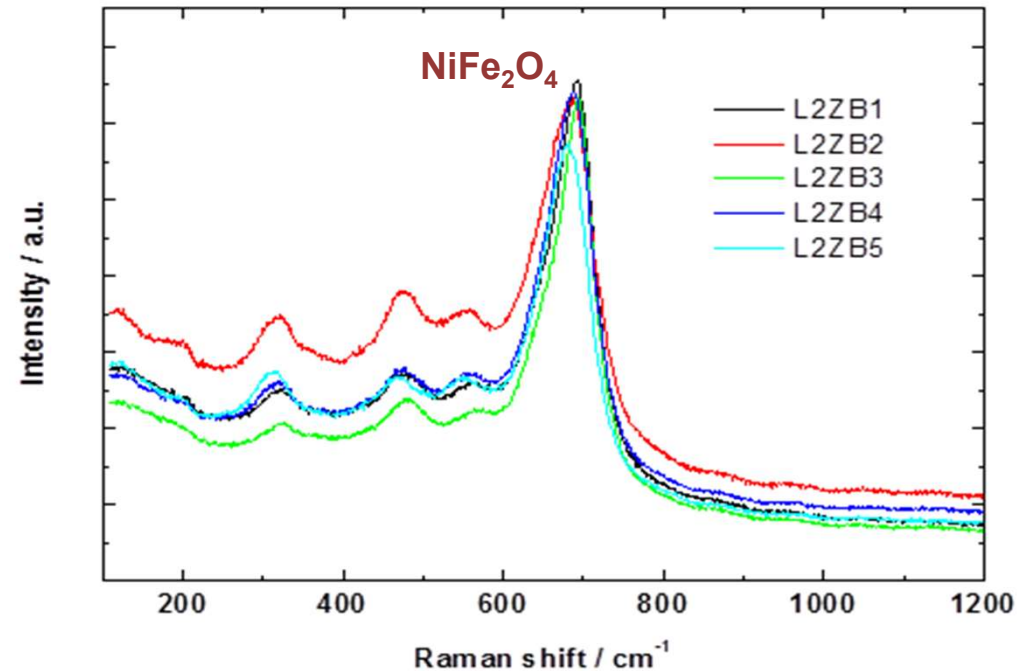
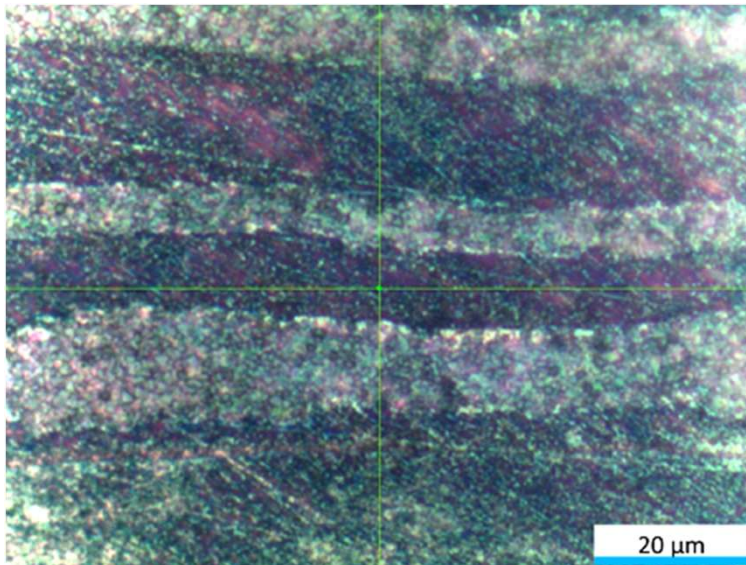


- The XPS analyses were firstly made at the outermost surface, revealing that the main elements were: O, C, Fe, Cr and Ni.
- The most probable species are Ni(OH)₂, Cr₂O₃ and Fe₃O₄, including possible (Fe, Cr) and (Fe, Ni) spinels.

spinel more probably
CrFe₂O₄ - NiFe₂O₄



- ❑ Oxide Surface Characterization by Raman Spectroscopy confirms the presence of mixed (Fe, Cr, Ni) spinel.
- ❑ The Raman spectrum is associated with inverse spinels : NiFe_2O_4 (i, ii)
- ❑ The higher the 700 cm^{-1} signals the higher the crystallite size could be.

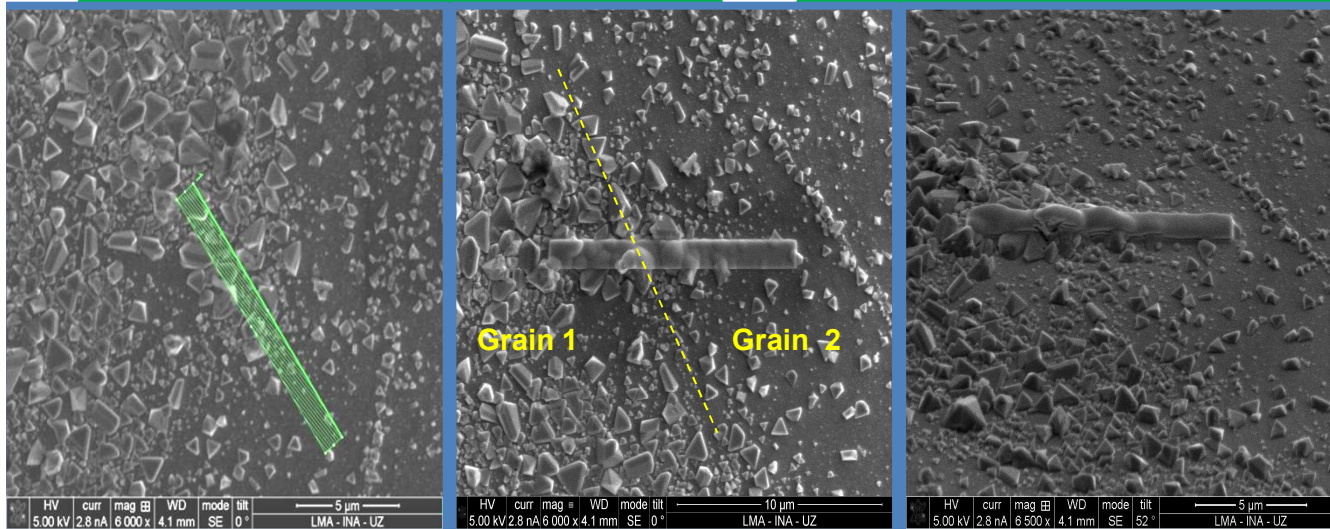


NiFe_2O_4 : 700 cm^{-1} (strong); 660 cm^{-1} (shoulder); 600 cm^{-1} (weak); 490 cm^{-1} (weak); 338 cm^{-1} (weak)

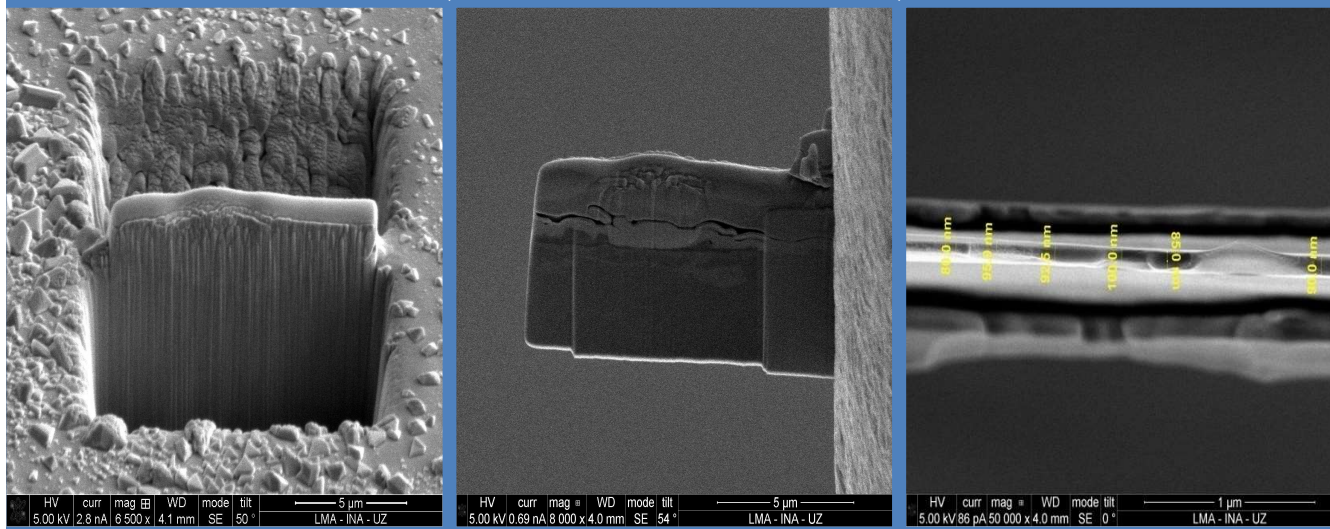
i. Froment, F., Tournié, A., Colombari, Ph., *J. Raman Spectrosc.*, 2008. 39: p. 560-568.

ii. Monnier, J., Bellot-Gurlet, L., Baron, D., Neff, D., Guillota, I., Dillmann, Ph., *J. Raman Spectrosc.*, 2010. 42: p. 773-781.

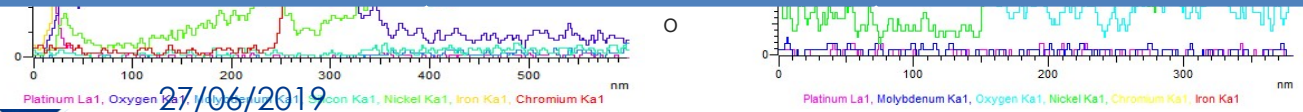
Results: REFERENCE CONDITIONS-TEM



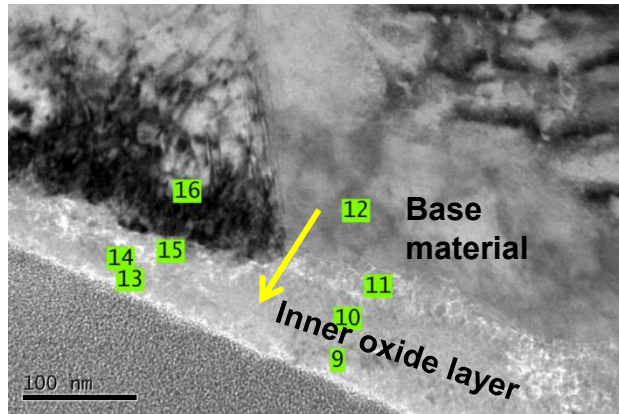
- Samples were prepared by FIB to study the cross-sectional oxide morphology
- EDX analysis was performed from the external surface to base material and across grain boundary penetration.



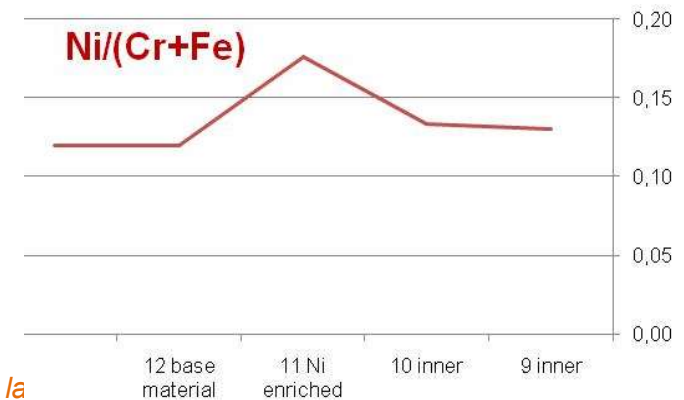
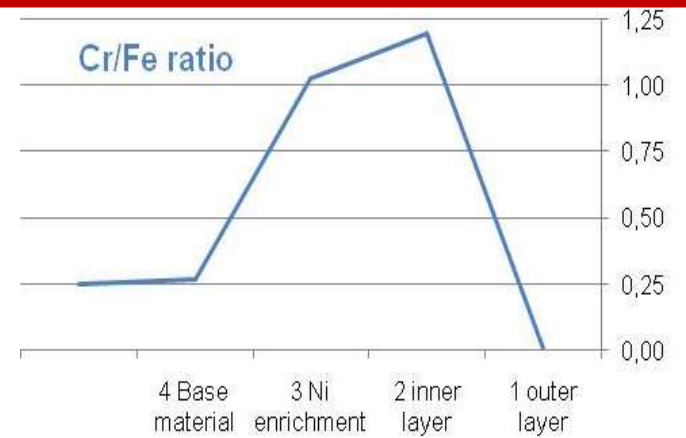
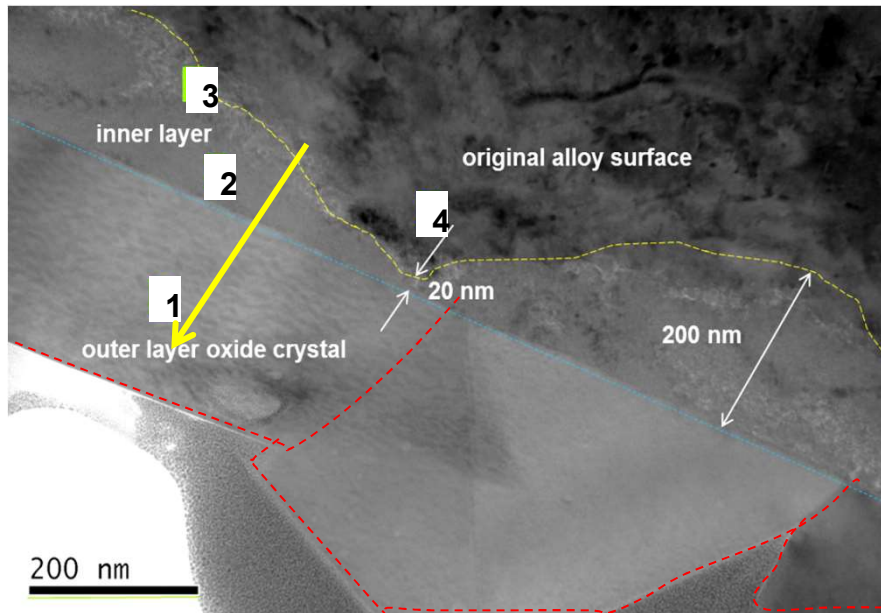
Ni enrichment was observed under inner layer and across grain boundary



Results: REFERENCE CONDITIONS-TEM



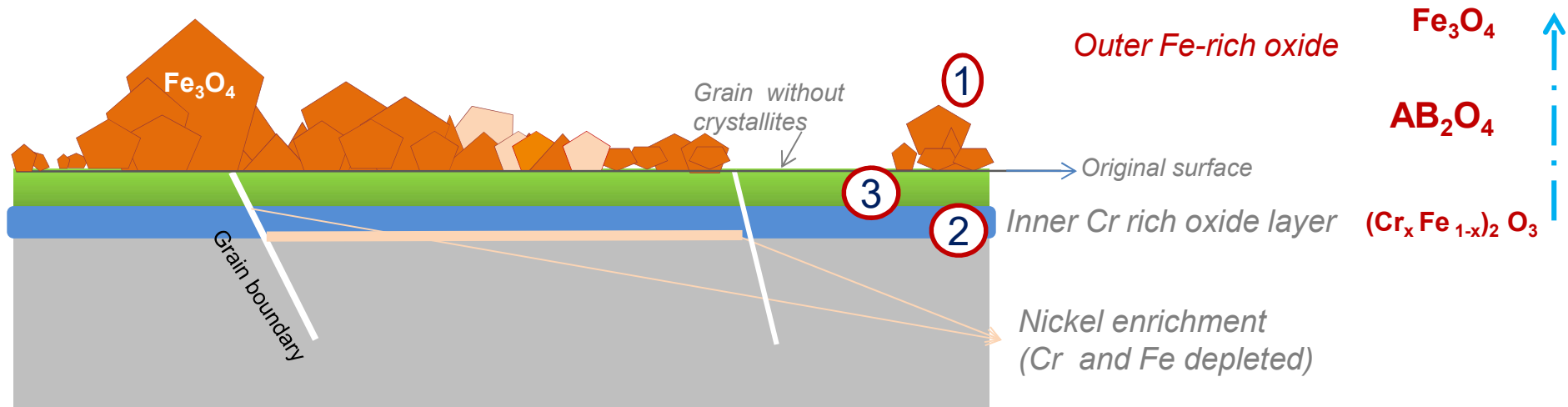
- Cr/Fe and Ni/(Cr+Fe) ratio were determined.
- Cr/Fe is **close to 1** in the inner layer ratio, this results support that the inner layer is formed by an FCC spinel ($\text{Cr}_{1.5}\text{Fe}_{1.5}\text{O}_4$)^{i, ii}
- The external oxide layer is composed by magnetite (Fe_3O_4)
- **Ni/(Cr+Fe) close to 0,18** indicates the Ni enrichment below the oxide layer.



ⁱ Soulas, R et al. (2013).. Journal of Materials Science. 48. 2861-2871.

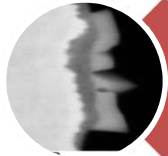
ⁱⁱ Couvant T, Vaillant F, Boursier JM, Delafosse D (2004) Eurocorr 2004, Nice



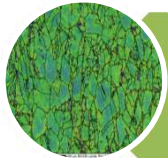


* Oxidation and cation release of stainless alloy in ligh water reactor. P. Combrade. ANT International (2015)

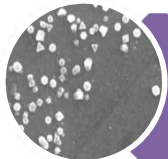
1. The **outer layer** is composed of large oxide crystallites Fe rich (Fe_3O_4)
2. The **inner layer** is compact. The Cr content in the inner oxide layer is similar to that in the matrix (Fe content is lower).
3. An **intermediate layer** of spinel AB_2O_4 was found. (CrFe_2O_4 and NiFe_2O_4)
4. The **thickness** of the inner oxide layer is heterogeneous, between 20 and 200 nm.
5. Higher oxide thickness is **detected** in some grain orientation.
6. **Nickel enrichment** is present under the inner layer and across grain boundary.



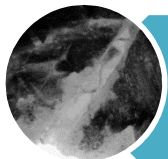
Surface finishing: if roughness increase, the heterogeneities on the surface are higher.



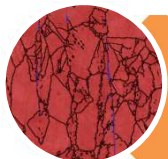
CW produces a significant increase in the dislocations density.



Environment changes can affect the structure and chemical composition of the surface oxide (B/Li ratio and transient condition) because the water chemistry had significant modifications in its environment.



Hydrogen atoms produced by radiolysis or redox reactions can travel through the surface of the material changing the structure of the oxide layer.



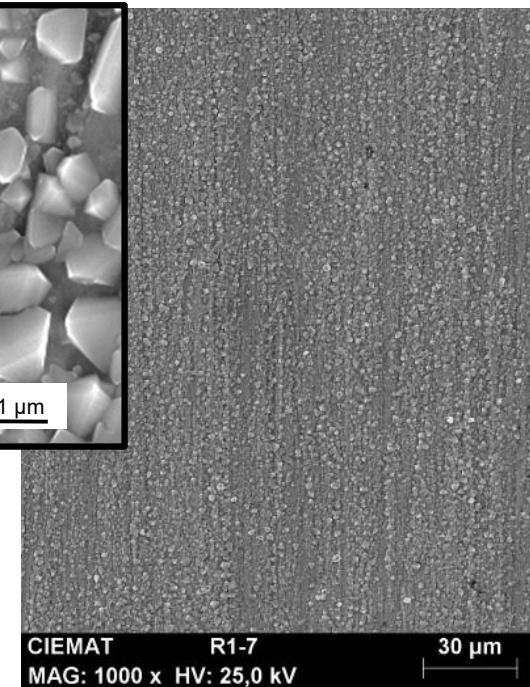
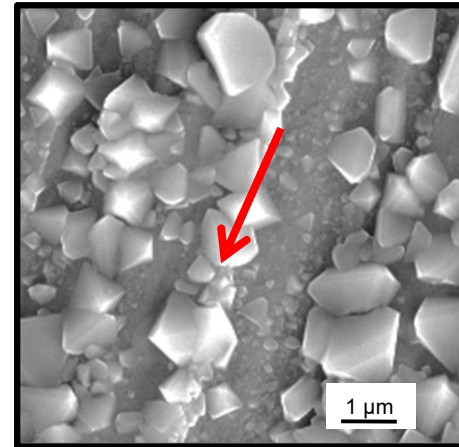
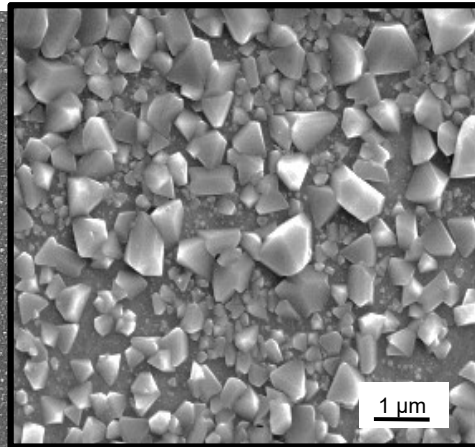
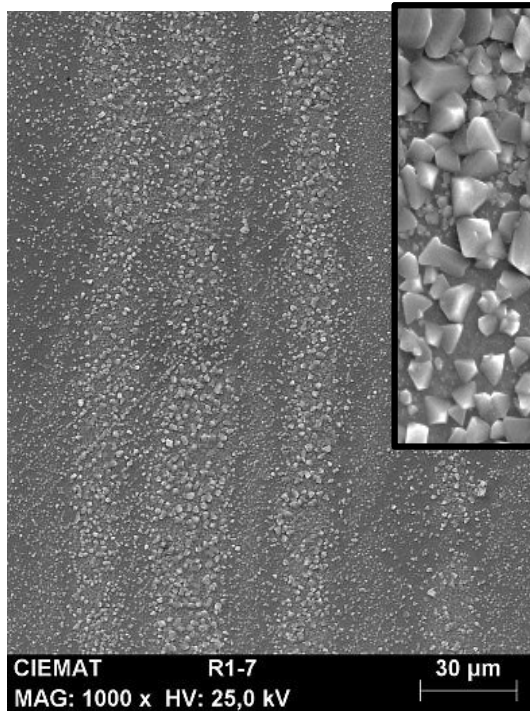
Heterogeneities: δ ferrite, grain boundary and twins produce different microstructure and composition of the oxide layer.

Surface finishing- 1000 h- Primary water



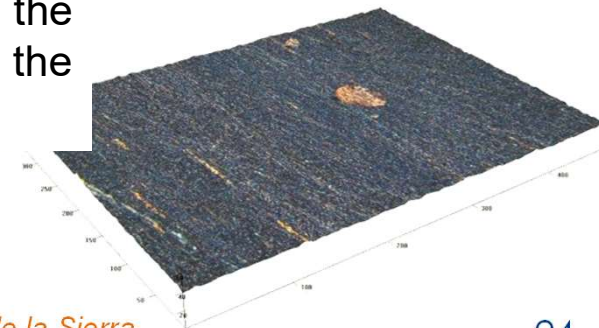
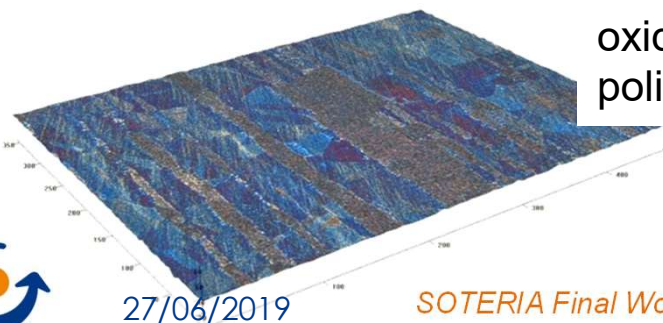
Polished side

Ground side



• The uniformity of the oxide surface was affected by surface preparation methods

• A ground surface finish produces heterogeneous growth of the oxide layer comparing to the polished.

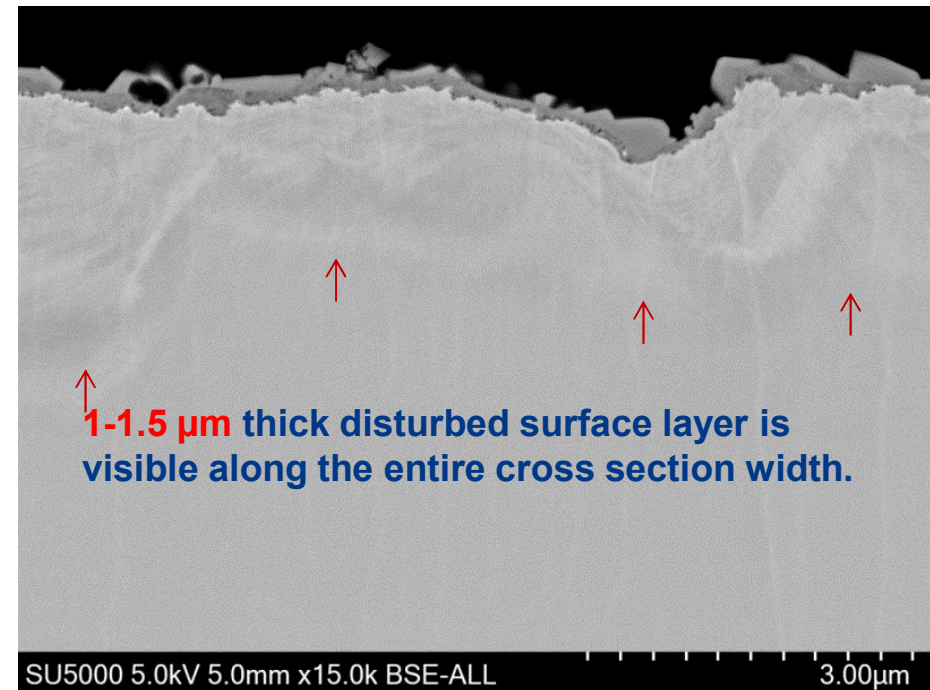
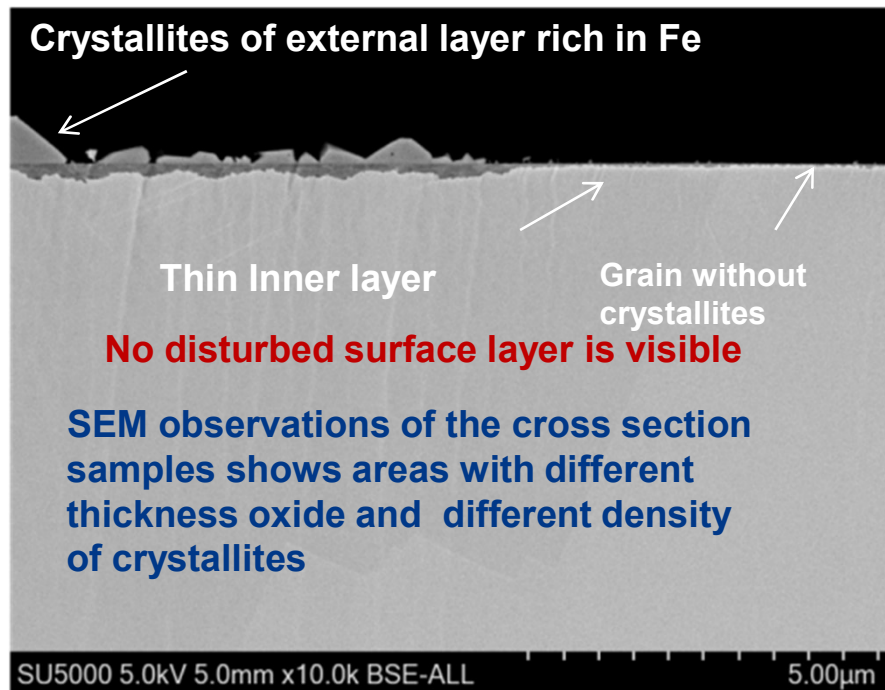


Surface finishing- 1000 h- Primary water



Polished side: Top surface is **perfectly smooth**

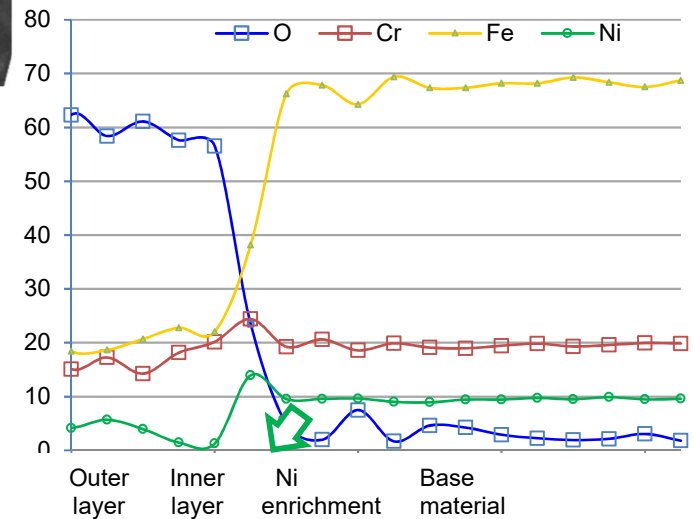
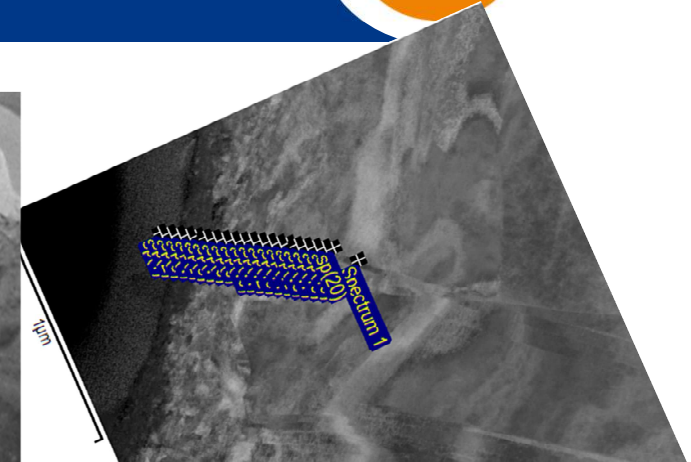
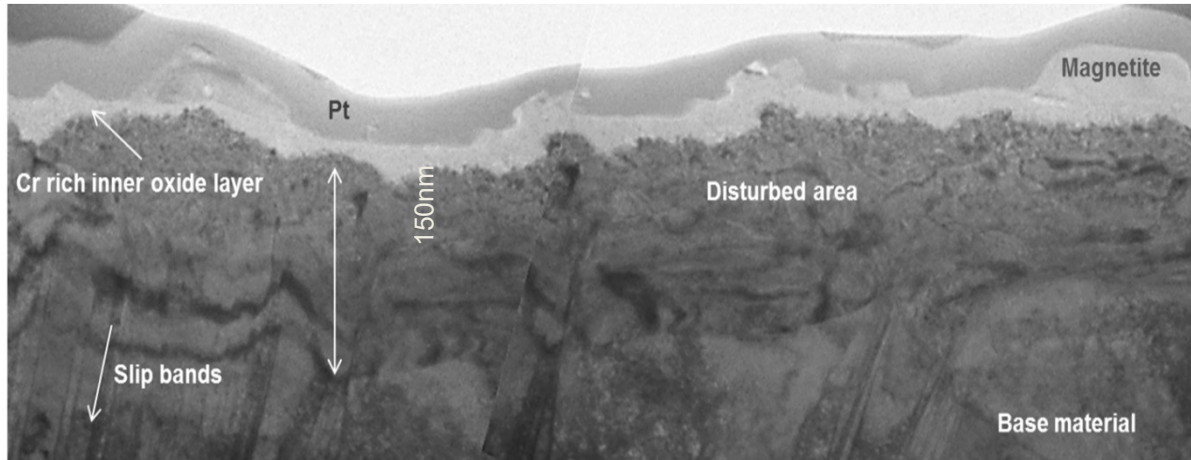
Ground side: Top surface is **very rough**



Lower roughness contributed to improved oxidation resistance



Surface finishing- 1000 h- Primary water



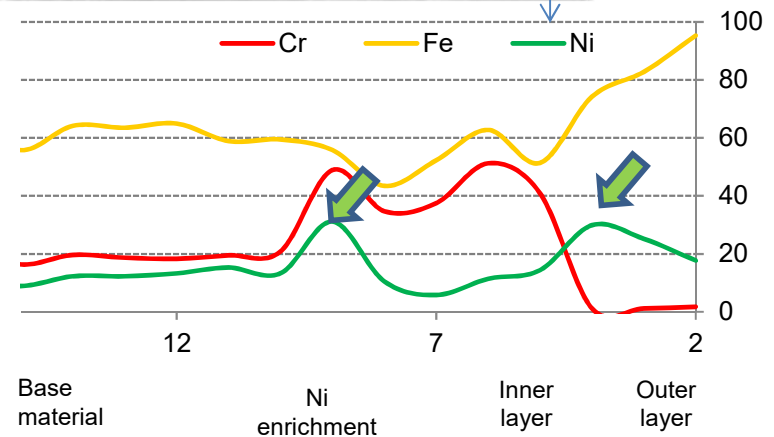
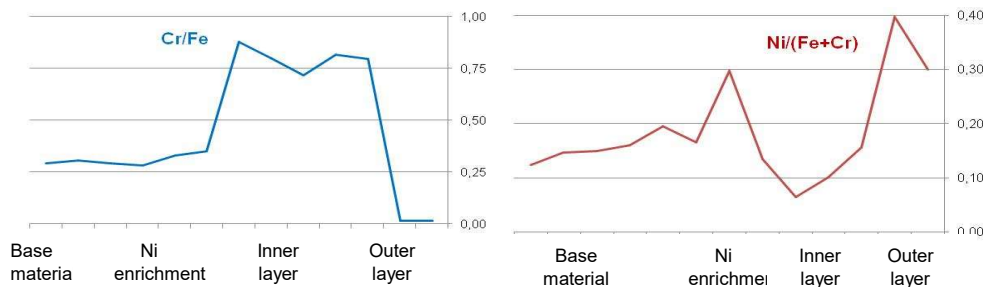
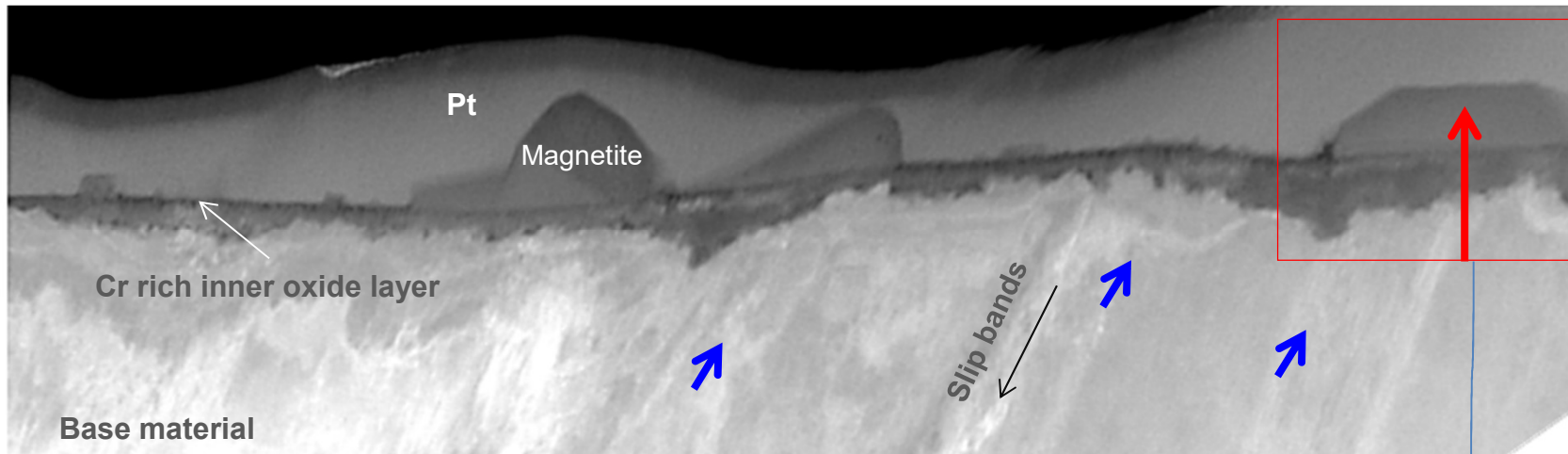
Defects may act as diffusion short-circuits for oxidizing species

The chemical composition of the oxide layer on the ground surface is different of the polished one. Ni and Cr are present in the outer layer.

Ni enrichment is also observed under the inner layer



Cold Worked Effect - 1000 h- Primary water

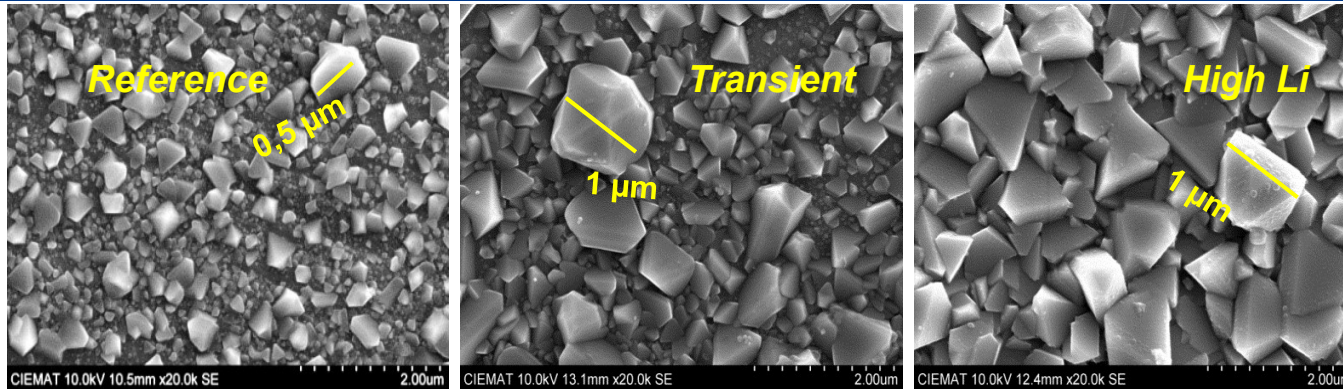


The composition of the oxide layer on the CW alloy is similar to the ground surface. Higher Ni are present in the outer layer too.

Slip band act as diffusion short-circuits for oxidizing species

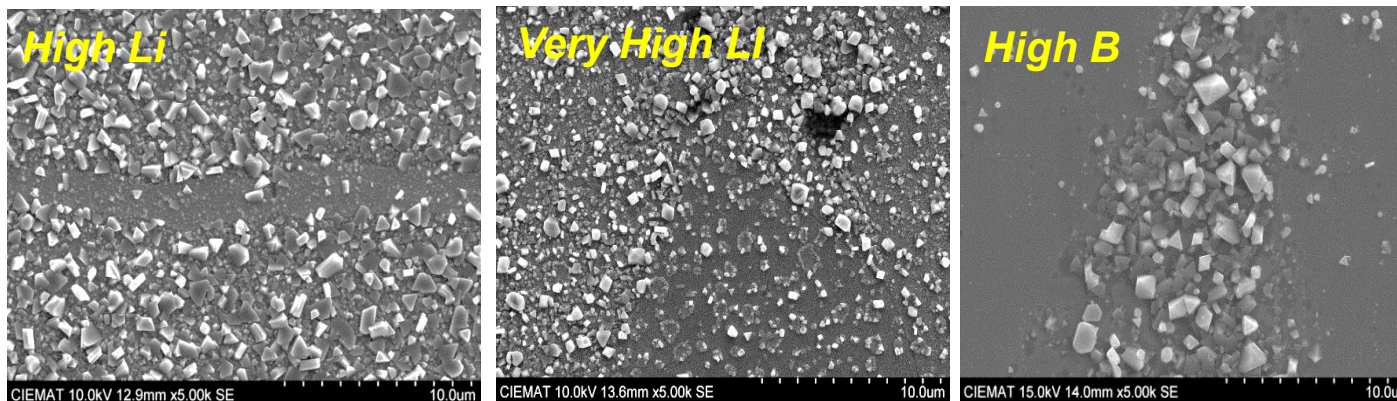
Ni is present under the inner layer and in the outer layer.

Environment: (B/Li ratio and Transient condition)



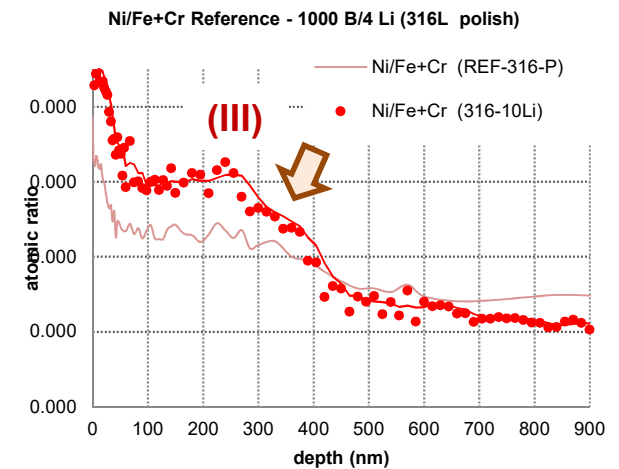
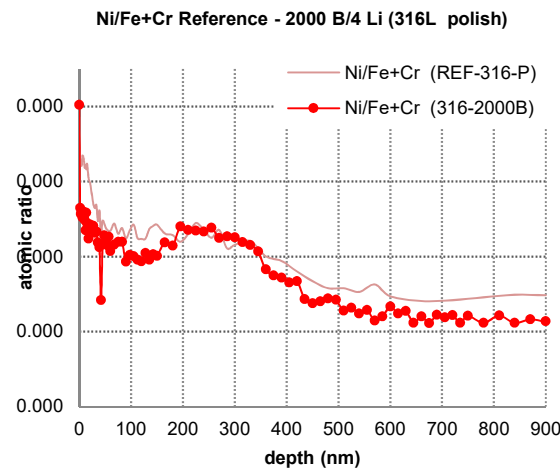
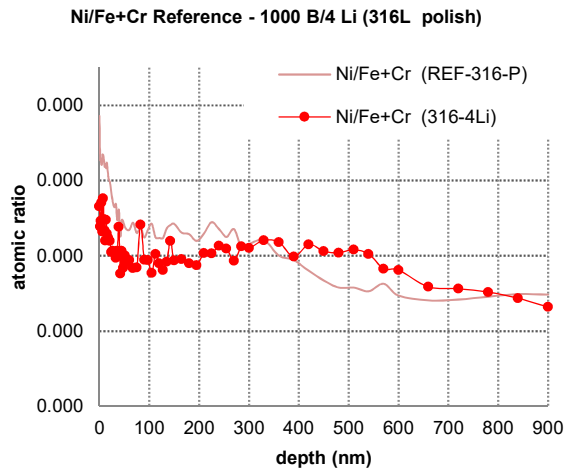
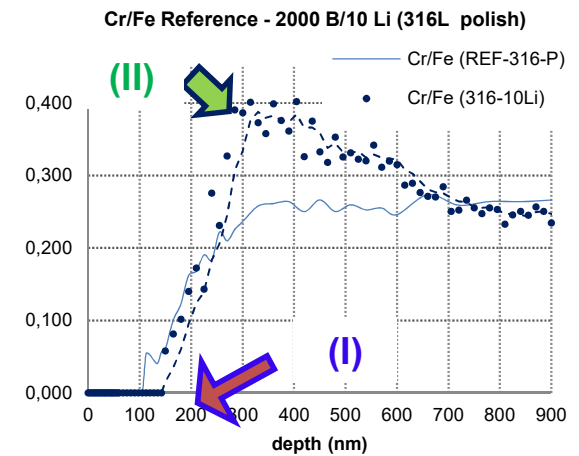
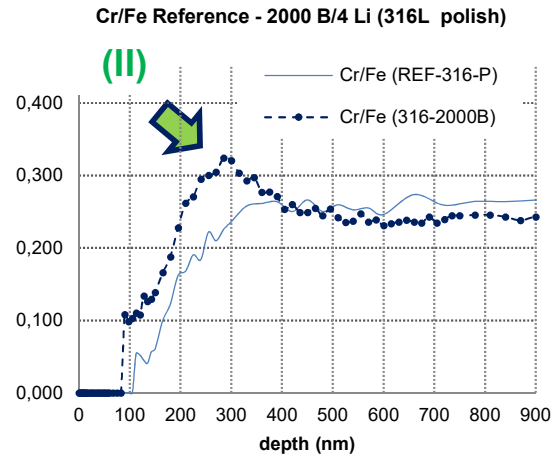
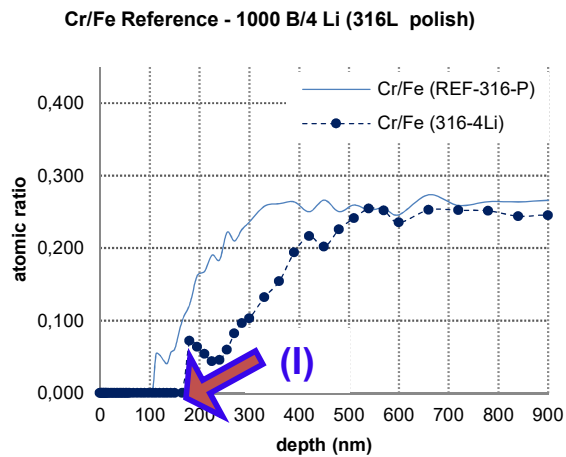
- Size of crystallites is lower in reference conditions
- Size Increase with lithium and in transient conditions

The higher the crystallites size is observed, the thicker the outer oxide layer is formed on the surface.



- Remarkable decrease in oxide layer thickness with increasing boric acid concentration (*)

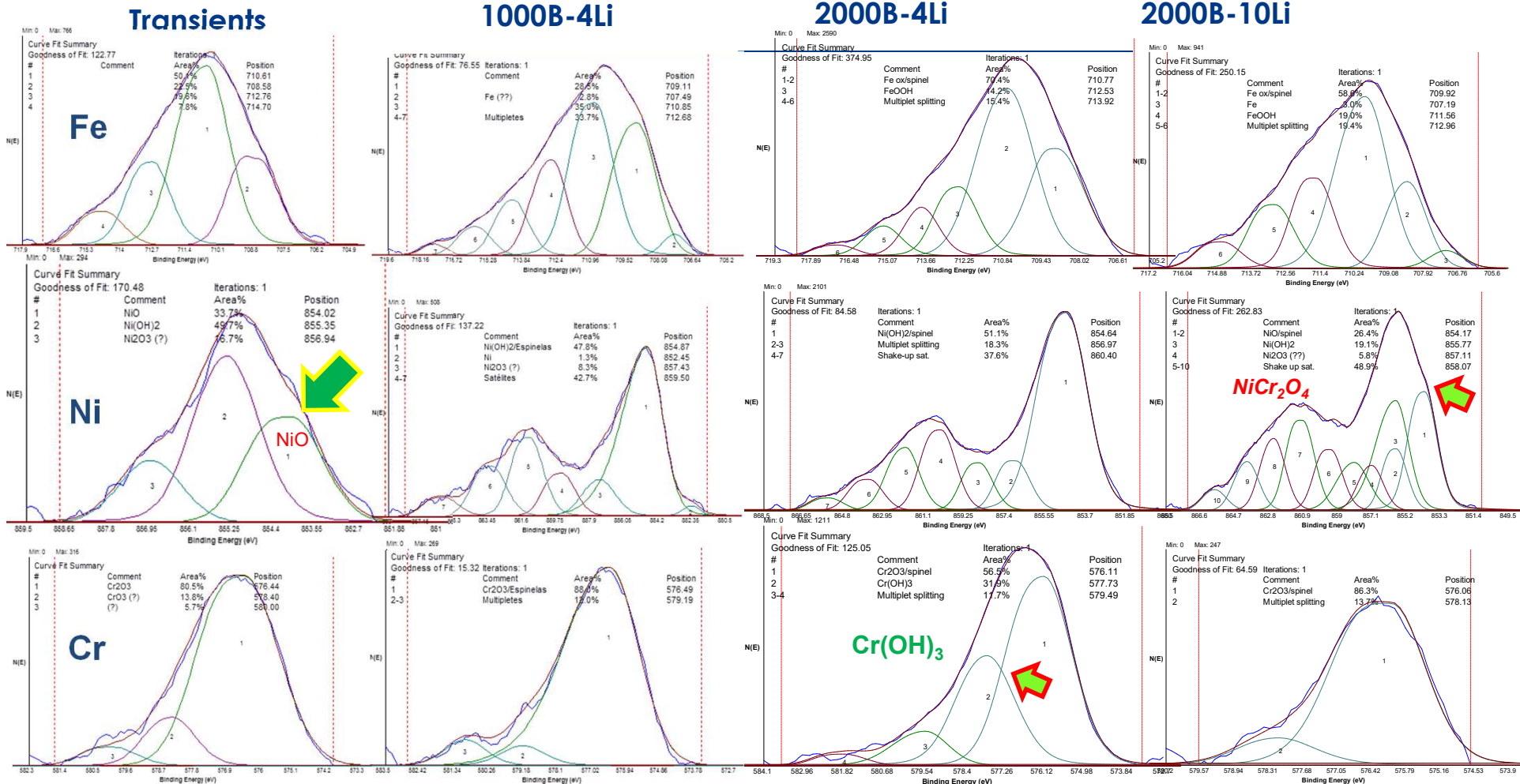
Environment: (B/Li ratio and Transient condition)



Auger Spectroscopy indicates that the different environments produce variations in the structure and chemical composition of the oxide layer. **(I) Samples tested in high Li environment show a thicker outer layer (Fe rich) than reference sample. (II) Cr/Fe ratio is higher in high B. (III) NiFe ratio is higher in high B & high Li.**



Environment: (B/Li ratio and Transient condition)



XPS spectra of the outermost surface for Fe, Ni and Cr regions at different conditions tests show the presence of Cr_2O_3 and Fe_3O_4 together with Fe-Ni spinels.

Only in transient conditions NiO is observed

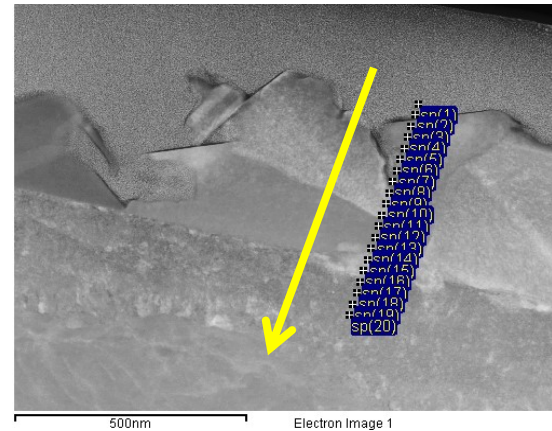
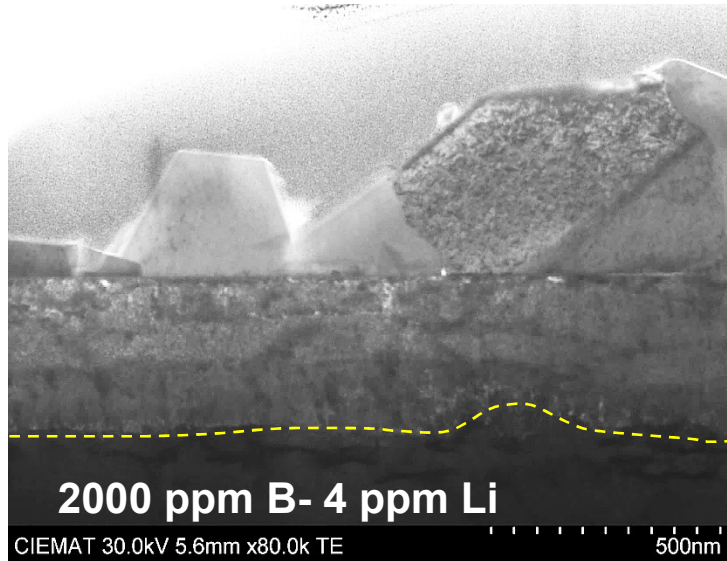
NiFe₂O₄ and Fe₂CrO₄ are the most likely in 1000B –4 Li and 2000B –4 Li environments

Only in 2000B –10 Li conditions NiCr₂O₄ appears

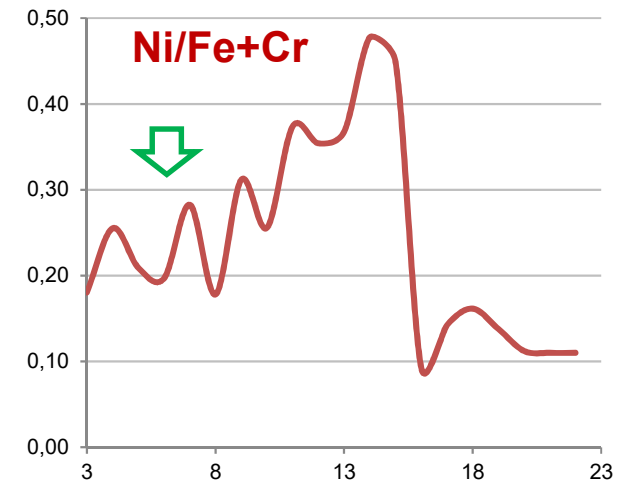
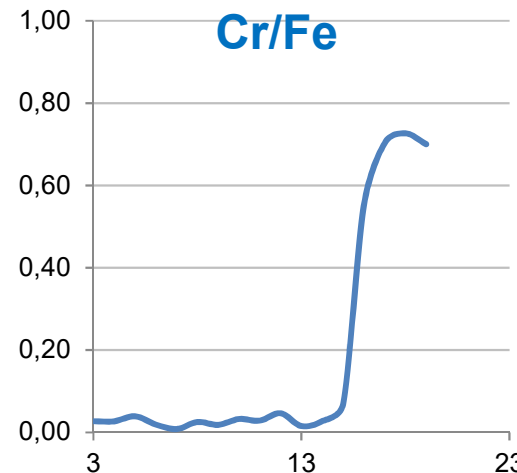
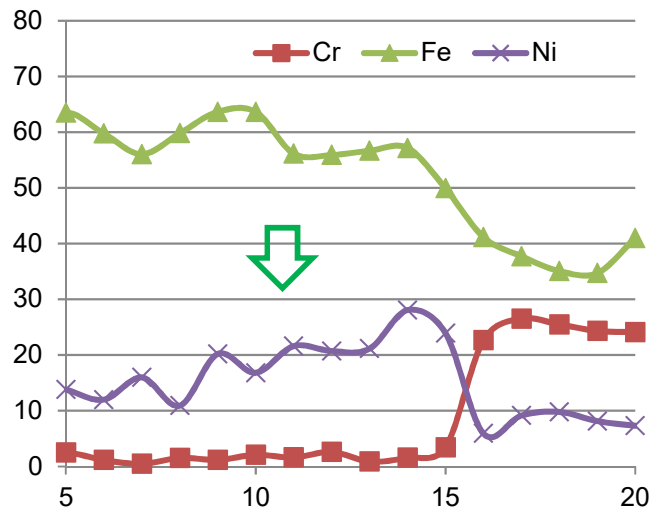
In 2000B –4 Li environments Cr(OH)₃ is detected



Environment: (B/Li ratio)

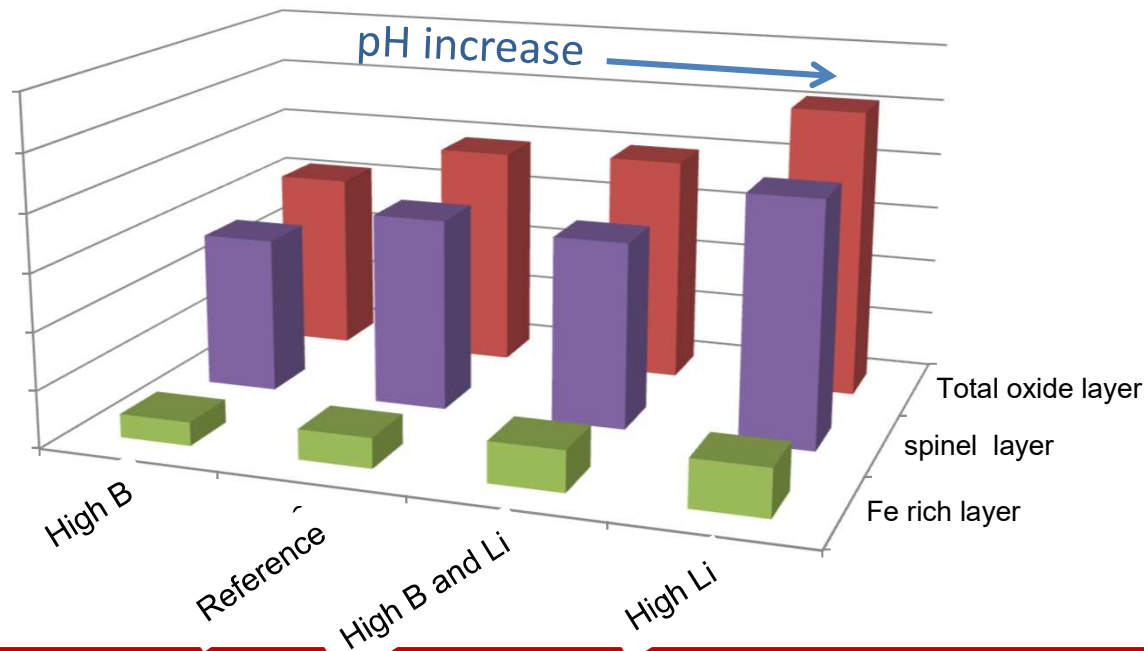


Very high Ni enrichment under the inner oxide layer indicates a different stoichiometry of the outer surface than reference samples.



The thickness of the different oxide layer was determinate from Auger, SEM and EDS analysis.

The thickness of the total oxide layer was estimated at the point at which iron concentration is the base material.



The thickness of the total oxide layer was estimated at the point at which the Cr begins to appear.

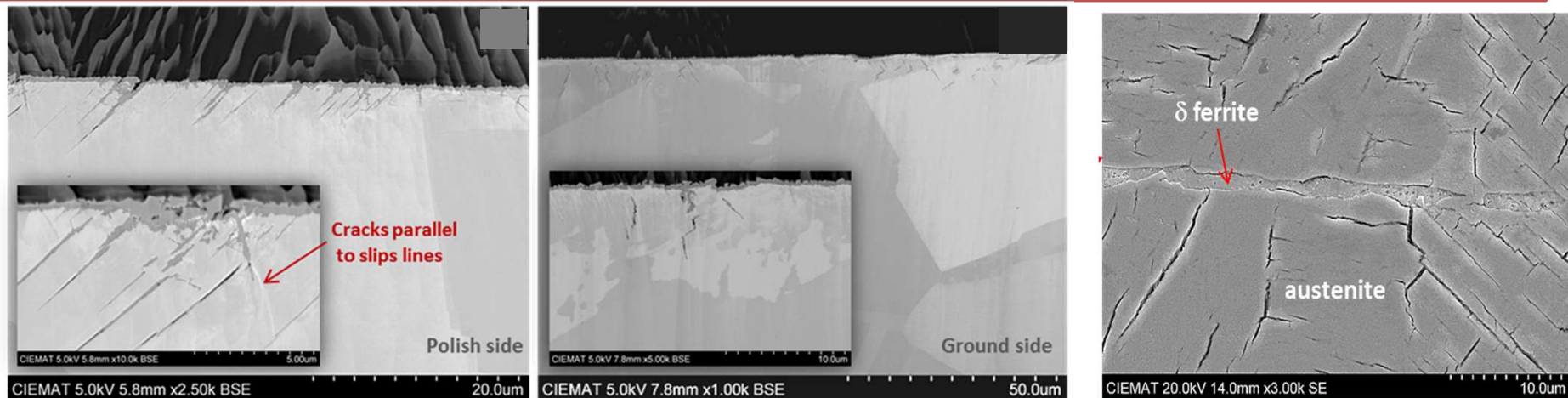
- Remarkable decrease in oxide layer thickness with increasing boric acid concentration (*)
- Remarkable increase in oxide layer thickness with increasing Li (pH)

* Arioka et al. 11th Int. Conf. Environmental Degradation of Materials in Nuclear System. Aug. 2003

Hydrogen charged + 1000 h- Primary water

- ❑ Residual and diffusible hydrogen was measured by hot extraction.
 - ❑ After cathodic hydrogen charging the **polished** samples contains **54 ppm** of hydrogen
 - ❑ In the **ground** sample the hydrogen decreases until **37 ppm**.
 - ❑ **After oxidation test** the hydrogen content is near to **0 ppm**.

Hydrogen is adsorbed into the crystal along the crystalline planes leading to produce cracking
(recombination $H+H \rightarrow H_2$)



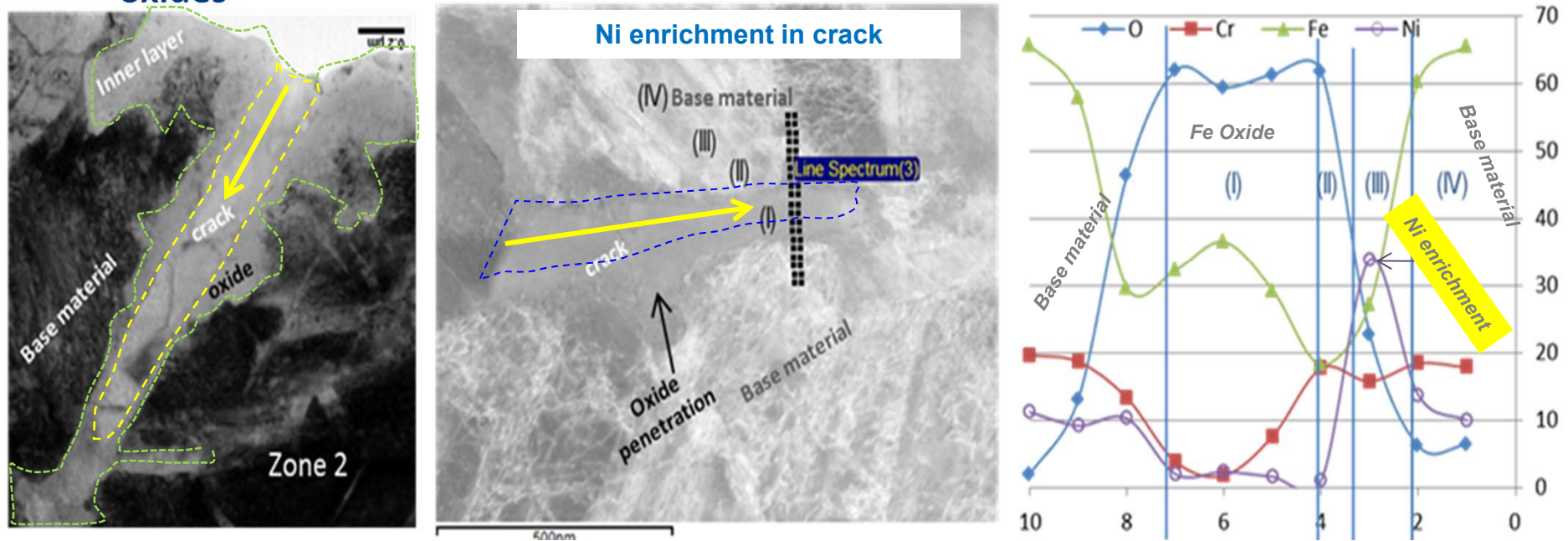
- ❑ Cathodic hydrogen charging leads to plastic deformation of the surface and produces a higher cracking in austenite than in δ ferrite. The two phases show a difference in plastic accommodation (*)
- ❑ The octahedral sites are more likely to hydrogen absorption than the tetrahedral ones (**)

(*) Gadgil V. et al. Scripta Metallurgica et Materialia (1993) 1489-1494

(**) Meng F. et al. Corrosion Science 53 (2011) 2558-2565

Hydrogen charged + 1000 h- Primary water

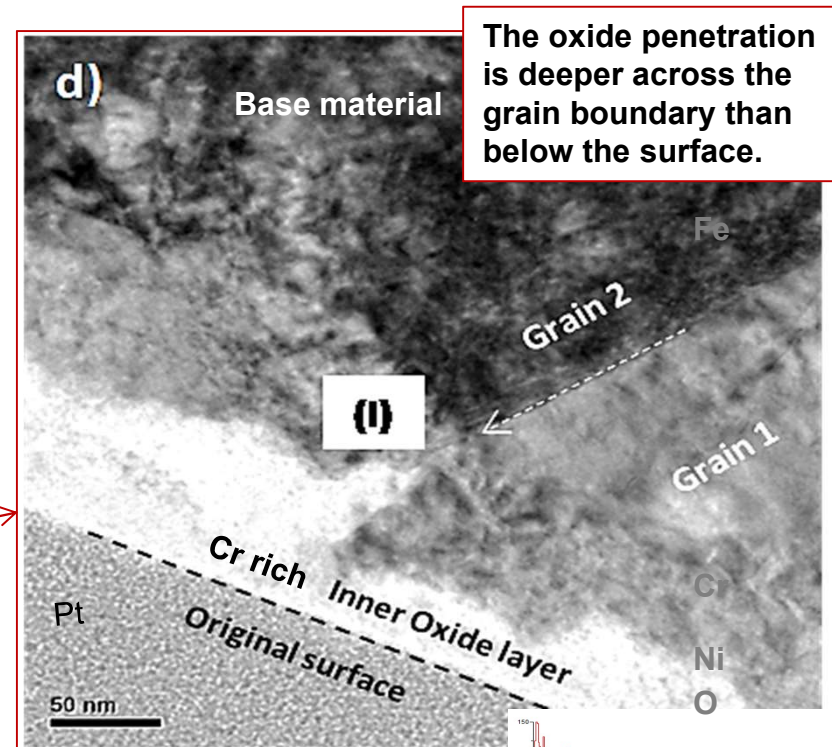
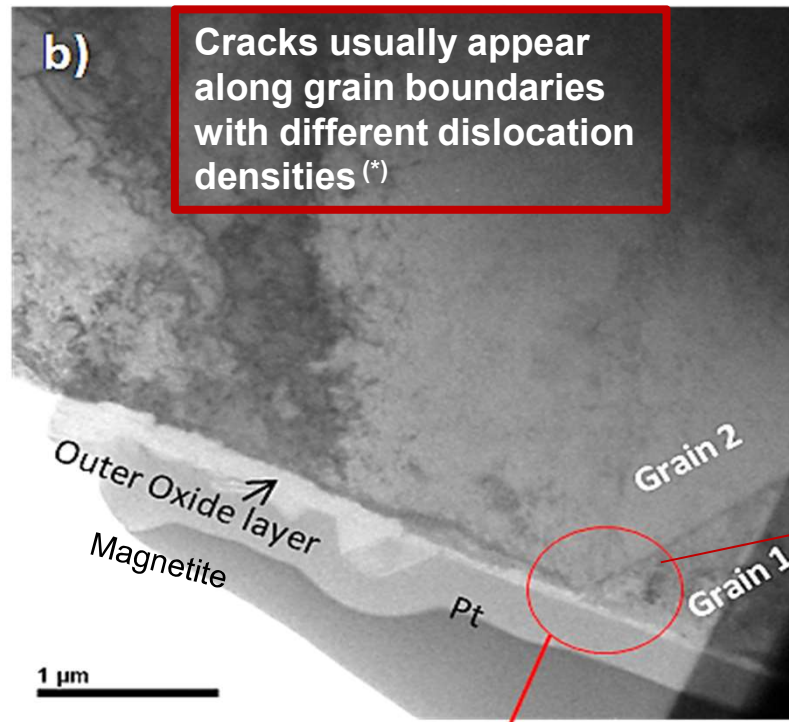
- Cross-section TEM image shows a crack formed during cathodic charge or hydrogen desorption. EDX analyses: *I) Fe rich oxide at the crack III) Ni enrichment IV) Base material*
 - Cracks were filled with Fe-rich oxide
 - Crack wall shows a Cr-rich penetration similar to the surfaces
 - Ni enrichment layer is also observed on both sides of the cracks
 - Hydrogen may be trapped in Ni-enriched (Cr-depleted) zones underneath surface oxidesⁱ



K. Kruska, D. W. Saxey, T. Terachi, T. Yamada, G. D. W. Smith, and S. Lozano-Perez. 16th International Conference on Environmental Degradation of Materials in Nuclear Power Systems - Water Reactors, I, 2013

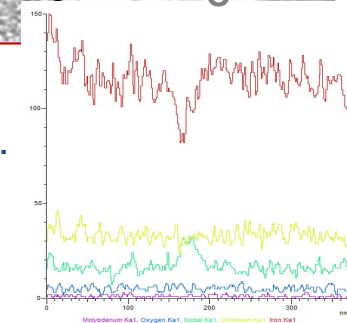
Heterogeneities: grain boundary

- The study of heterogeneities in the material plays an important role to detect the growth of the oxide layer through them.

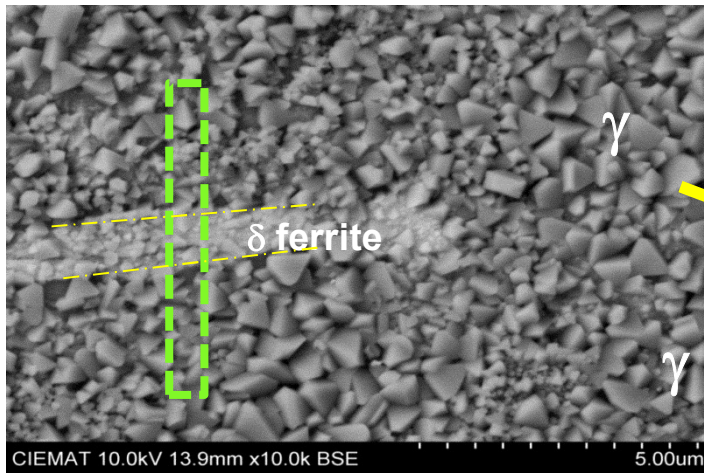


- Ni enrichment is observed across the grain boundary by EDS analysis.

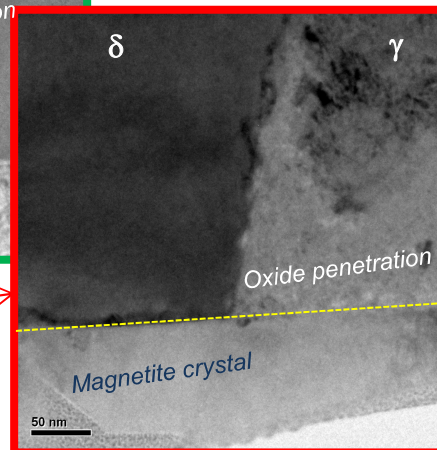
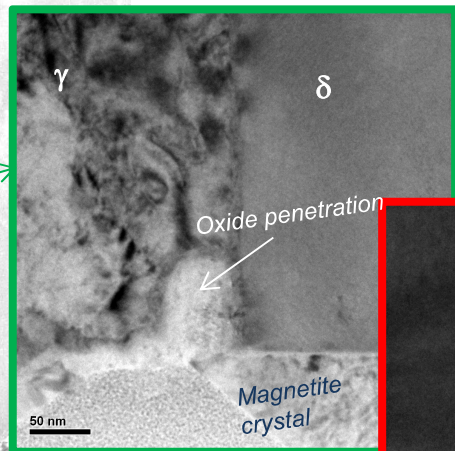
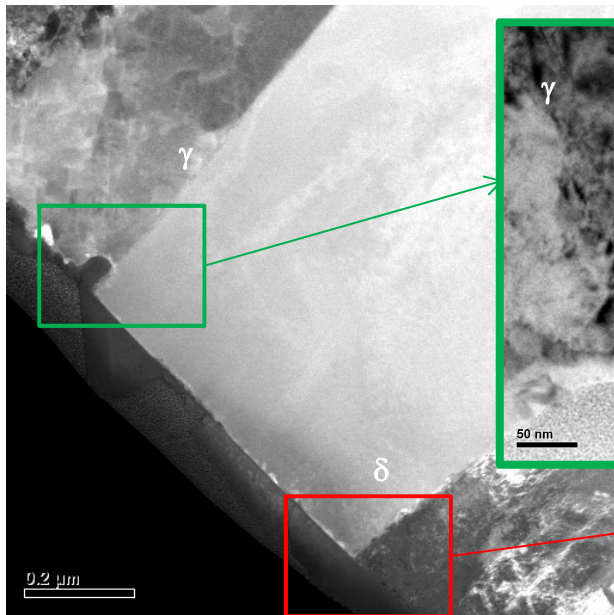
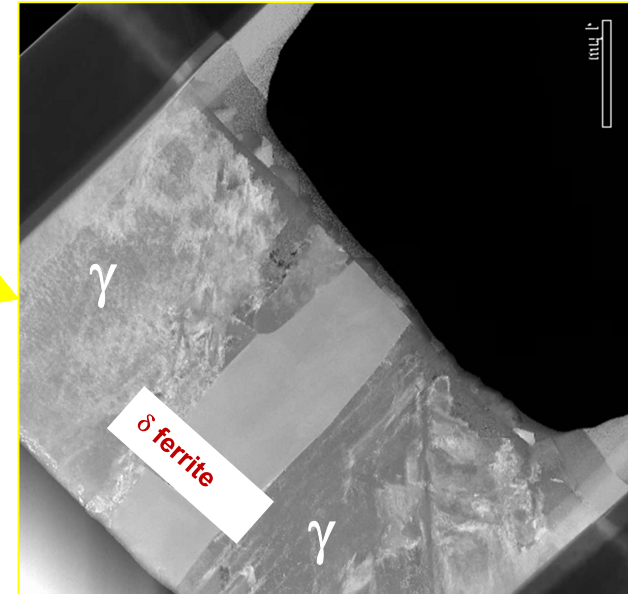
(*) Herbelin, A. et al.e, Gabriel. (2010). Oxidation of austenitic stainless steels in PWR primary water. (2015)



Heterogeneities: δ ferrite



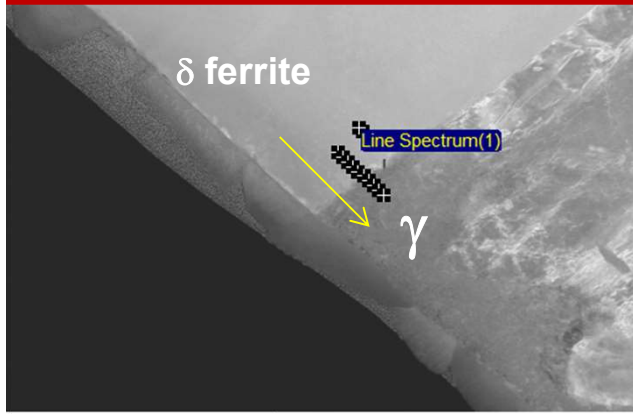
FIB



The oxide layer seems to penetrate deeper through microstructural defects (interface γ - δ).

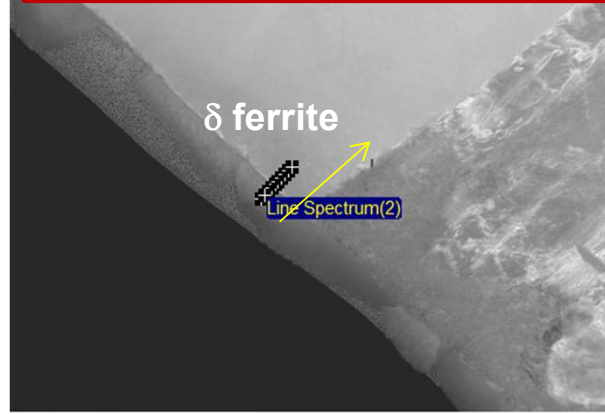
Heterogeneities: δ ferrite

Ni enrichment across grain boundary



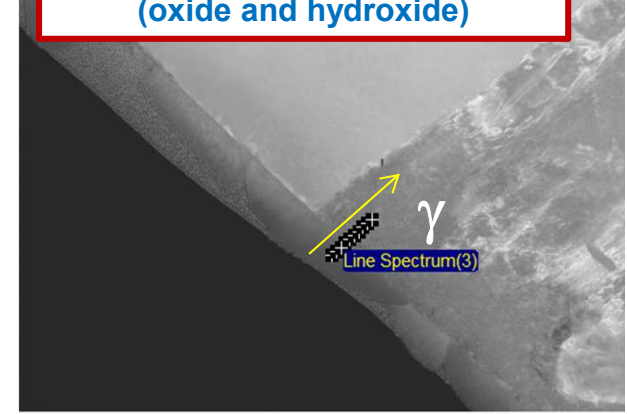
500nm

Ni enrichment: below Cr rich layer

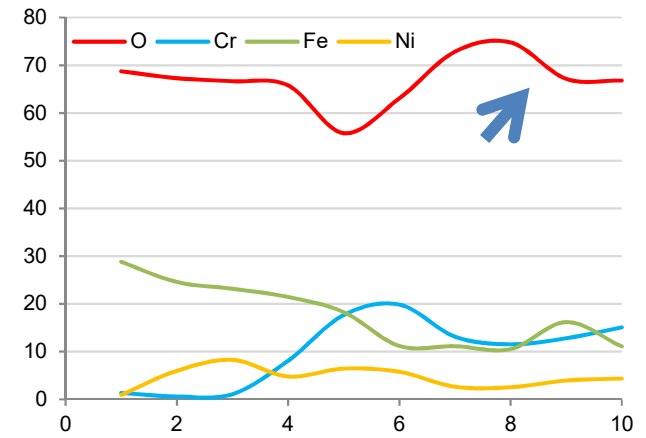
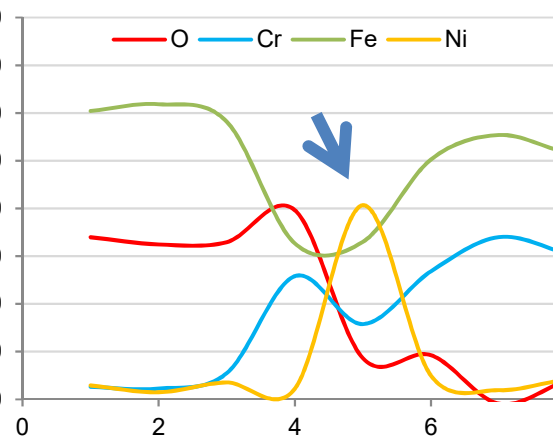
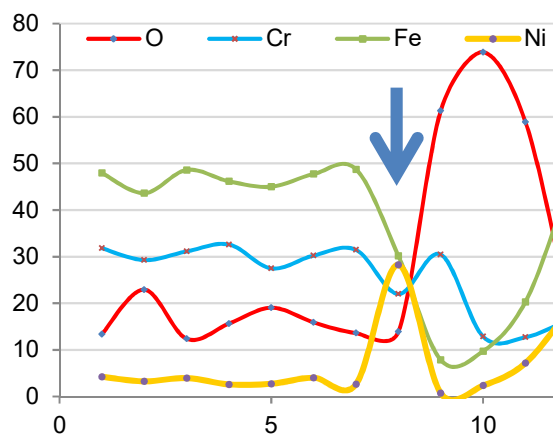


500nm

Very high oxygen in austenite (oxide and hydroxide)



500nm



- Less oxidation is observed in δ ferrite than austenite.
- Ni rich-region could act as a barrier for oxygen diffusion and oxide growth (*)

(*) Kruska K. et al. Corrosion Science 63 (2012) 225-233



4. Summary



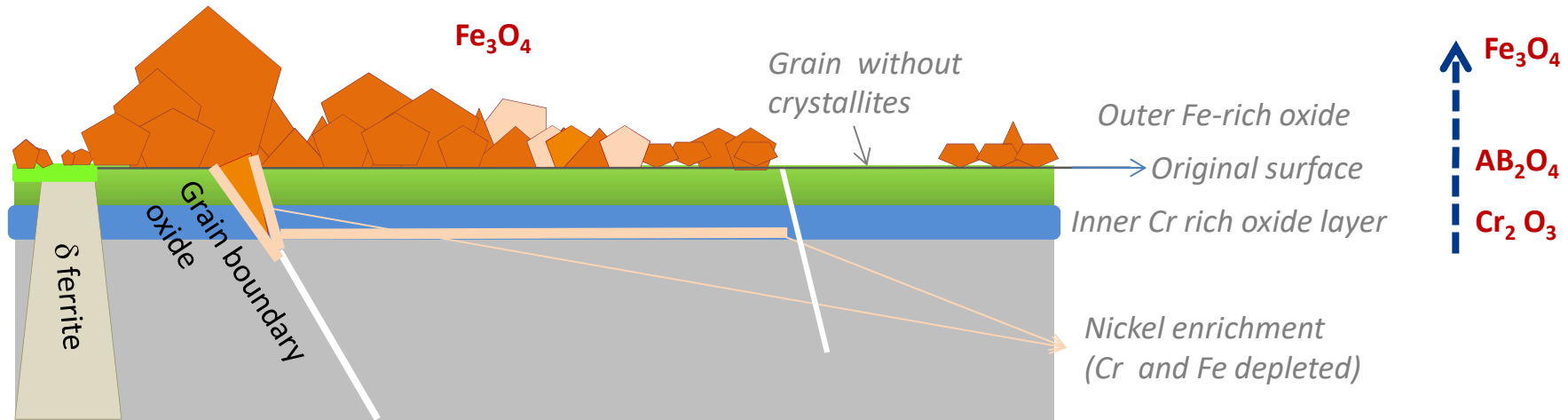
Summary



- ❑ Different environments and different finish surface modify the thickness and chemical elements distribution of the oxide layer formed in simulated PWR.
- ❑ EBSD analysis previous to oxidations tests helps to select specific areas to determine the composition through another techniques AES, XPS, Raman and TEM
- ❑ The effect of **cold worked** and ground finished surface produce a higher nickel enrichment than reference condition in the oxide/metal interface. Ni rich-region could act as a barrier for oxygen diffusion and oxide growth.
- ❑ Increases the dislocations density in the microstructure (CW, surface finish and/or hydrogen) produce a detrimental effect on the protective layer, leading to the increase of Fe_3O_4 on the surface.
- ❑ **Heterogeneities** on the oxide surface are clearly identified and are associated with different phases and orientations of the grains.



Structure proposed



The protective oxide layer formed in SS plays a very important role in corrosion resistance.

This oxide layer evolves depending on the environment and can be lost the protective character. $Cr_2O_3 \rightarrow AB_2O_4 \rightarrow Fe_3O_4$

- Higher outer oxide thickness is observed in high Li
- Spinel Nickel rich on the surface is observed in very high Li
- A deeper penetration of the oxide layer due to the heterogeneities
- High oxide penetration due to the deformation and CW

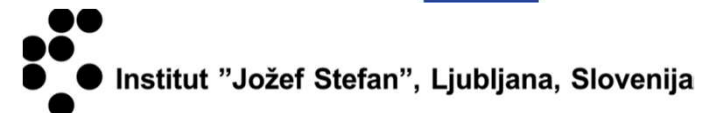
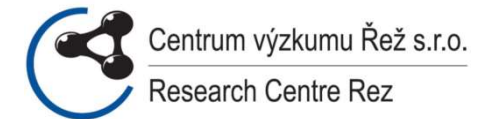
The quantification of all of these effects must be conducted to complete the model. Results obtained from XPS, Auger and EDS will be reported in the deliverable.



thanks for your attention



The SOTERIA Consortium



The SOTERIA Contacts



The SOTERIA Project Coordinator

Christian ROBERTSON
CEA
christian.robertson@cea.fr

The SOTERIA Project Office

Herman BERTRAND
ARTIC
bertrand@artic.eu

www.soteria-project.eu

This project received funding under the Euratom
research and training programme 2014-2018
under grant agreement N° 661913.

